Research Article

Reconstructing Holocene fire records using dune footslope deposits at the Cooloola Sand Mass, Australia

Nicholas R. Patton[a,b,c] (iD), James Shulmeister[a,b], Quan Hua[d], Peter Almond[e], Tammy M. Rittenour[f],
Johanna M. Hanson[a], Aloysius Grealy[b], Jack Gilroy[b] and Daniel Ellerton[b,g]

[a]School of Earth and Environment, University of Canterbury, Christchurch 8041, New Zealand; [b]School of Earth and Environmental Sciences, University of Queensland, Brisbane 4072, Australia; [c]Desert Research Institute, 2215 Raggio Parkway, Reno, Nevada 89512, USA; [d]Australian Nuclear Science and Technology Organisation, Kirrawee DC, New South Wales, 2232, Australia; [e]Department of Soil and Physical Sciences, Lincoln University, Christchurch 7647, New Zealand; [f]Department of Geosciences, Utah State University, Logan, Utah 84322, USA and [g]Department of Geological Sciences, Stockholm University, SE 10961 Stockholm, Sweden

Abstract

In this study, we assess charcoal records from eolian deposits within the Cooloola Sand Mass, a subtropical coastal dune system in eastern Australia, to determine whether they can be used as a proxy for Holocene fire history. We excavate four profiles in depositional wedges at the base of dune slipfaces (footslope deposits) and calculate charcoal concentrations for three size classes (180–250 μm, 250–355 μm, and 355 μm–2 mm) at predetermined depth intervals. Age–depth models are constructed for each profile using radiocarbon measurements (n = 46) and basal optically stimulated luminescence ages (n = 4). All records appear intact with little evidence of postdepositional mixing as demonstrated by minimal age reversals and consistent trends in charcoal concentration and accumulation rates (CHAR) among size classes. Combining all four records, we generate a ca. 7 cal ka BP terrestrial fire history that depicts distinct peaks representing periods of increased local fire activity at <0.3, 1.1–0.4, 2.2–1.6, 3.4–2.6, and 6.7–5.3 cal ka BP. Our findings parallel regional records and highlight the utility of dune footslopes as ecological and sedimentary archives. As dune fields are much more common than wetlands and lakes in semiarid and arid areas, these deposits have the potential to increase the spatial resolution of fire records globally.

Keywords: Paleofire; Fire history; Charcoal; CHAR; Hillslopes; Eolian sediments; Sediment transport; Erosion; Colluvial; Landscape evolution

(Received 5 October 2022; accepted 9 March 2023)

INTRODUCTION

Wildfires are prevalent across much of the world; however, fire records are primarily limited to regions with abundant aquatic archives (e.g., Power et al., 2008; Harrison et al., 2022). As a result, identifying a potential sediment deposit commonly found within these areas, such as drylands, would provide a valuable target for paleoclimate studies and a means to evenly distribute fire records globally. The goal of this study is to assess the utility of dune footslope deposits to reconstruct fire histories. As a case study, we focus on stabilized Holocene dunes at the Cooloola Sand Mass (CSM) within the southeast (SE) Queensland dune fields (Fig. 1). The dunes are well dated (Walker et al., 2018; Ellerton et al., 2020; Patton et al., 2022b), their evolution is well understood (Levin, 2011; Patton et al., 2022a), and there are several aquatic records that can be used for comparison and validation (Donders et al., 2006; Mariani et al., 2019; Hanson et al., 2023). Specifically, the main objectives were to (1) assess whether sites

contain stratigraphically intact units with preserved depositional charcoal for developing a fire record; (2) evaluate the sensitivity of the records to charcoal size classes; (3) place the spatially aggregated charcoal records into the context of other records found in the SE Queensland dune fields; and (4) consider improvements to the data gathering and/or interpretation techniques. The outcomes will aid in the development of charcoal records from areas where fire is a rare event (wetlands/lakes) into regions where fire may be the dominant geomorphic and ecological process.

Fire in the Australian landscape

Fire is one of the most dominant landscape disturbances on Earth (Hennessy et al., 2005; Bowman et al., 2009; McLauchlan et al., 2020). This was clearly demonstrated in the 2019–2020 Black Summers bushfires in Australia, which burned ~240,000 km², destroyed more than 3000 houses, killed an estimated 1 billion animals, and displaced thousands of people (DAWE, 2020; Filkov et al., 2020; Richards et al., 2020; Canadell et al., 2021; Gallagher et al., 2021; Fig. 1). Fire activity (both frequency and severity) has been projected to increase due to changes in land use and climate (McKenzie et al., 2004; IPCC, 2021). It is therefore imperative to understand the role, frequency, and intensity
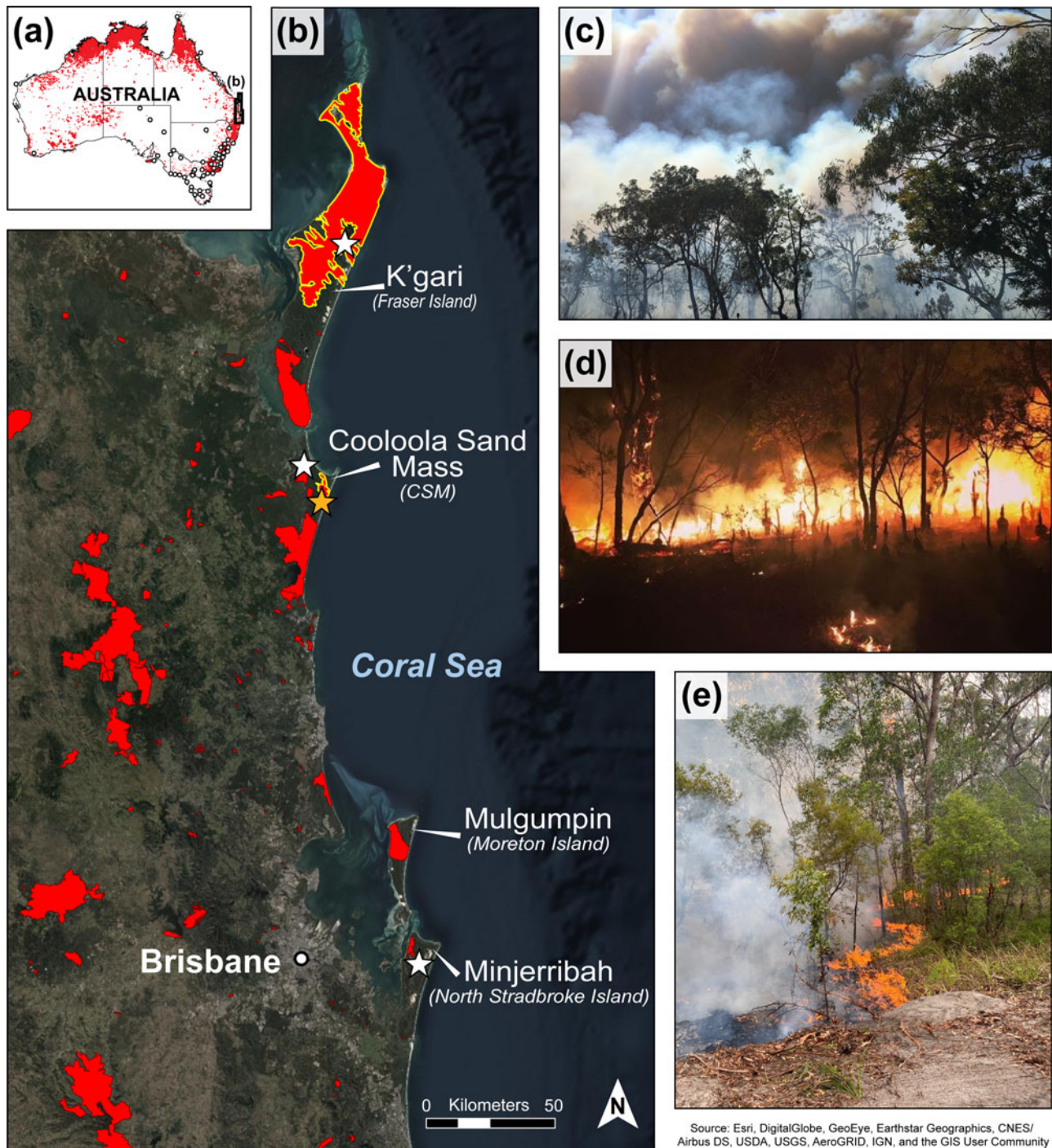
Figure 1. (a) Total area burned in Australia during the 2019–2020 Black Summers bushfires (red area) (DAWE, 2020) and the locations of sediment cores (white dots) used to generate Late Quaternary fire records in Mooney et al. (2011). (b) Satellite imagery of the SE Queensland dune fields and location of fires during the 2019–2020 fire season with the yellow outlines representing the Fraser Fire and Freshwater Road Fire on K'gari and the Cooloola Sand Mass (CSM), respectively. The orange star marks the field site for this study, whereas the white stars indicate the locations of fire records used for comparative purposes in this research. Images of (c) the Kings Bore Wildfire, (d) the Thannae Fire, and (e) the Freshwater Road Fire are provided as examples of wildfires that occurred within the SE Queensland dune fields during the Black Summers. Photo credits: (c) Michael Ford; (d and e) Erin Atkinson.

of fire in Australia, as it is one of the world's most fire-prone landscapes (Bradstock et al., 2002; Russell-Smith et al., 2007; Bradstock, 2010; van der Werf et al., 2017) and one that has a long legacy of both natural and anthropogenic fire occurrence.

Before the arrival of humans ca. 70–65 ka, evidence of fire in sedimentological records is intermittent and sparse and is presumed to be of minor importance in Australia (Singh et al., 1981; Moss and Kershaw, 2000; Clarkson et al., 2017). After this period, the subsequent substantial increase in fire activity is commonly ascribed to Indigenous arrival (Kershaw, 1986; Turney et al., 2001) due to their frequent use of small, low-intensity fire across the landscape, aka "fire-stick farming"

(Russell-Smith et al., 1997; Bowman, 1998). However, more recent studies have suggested little evidence of variations in fire regimes after human arrival, instead ascribing increased fire activity to changes in climate (e.g., Mooney et al., 2011).

The relationship between humans and fire is difficult to address in sedimentological records, because the timing of initial human arrival is not precisely known and there are autocorrelations between climate, vegetation, and fire (Bowman, 1998; Archibald et al., 2013). Not until European arrival and a shift to fire suppression and cessation in the last 200 yr, do we see a clear anthropogenic signal (Moss et al., 2011, 2015; Hanson et al., 2022). Indeed, the transition from traditional fire management to fire suppression is inferred to be responsible for not only increased fire severity, but also a shift in vegetation structure, boundaries, and community composition (Thompson and Moore, 1984; Pyne, 1998; Fletcher et al., 2021; Mariani et al., 2022; Stone et al., 2022).

Regardless of its origin, the role of fire in controlling Australian ecosystems and landscapes is widely accepted as significant (Bowman, 1998). There are large and growing paleofire data sets (e.g., Marlon et al., 2015; Gross et al., 2018; Hawthorne et al., 2018; Harrison et al., 2022), but the records in these databases are strongly biased toward wetland areas, and consequently, for Australia, there is a strong emphasis on the SE region (Fig. 1a). To broaden the coverage of fire histories, there is a need to extend records beyond peat bogs, swamps, and lakes; however, much of the Australian landscape is not suitable to sustaining long-term organic records (Bridgman and Timms, 2012; Chang et al., 2014, 2017), and finding suitable sites for the preservation of sedimentary charcoal is therefore challenging (e.g., Leys et al., 2018). As a result, there are spatial discrepancies in data coverage across the continent, particularly in the interior and in the tropics and subtropics. A means to extend fire histories to the continental interior, where fires may be the dominant ecological process, is needed. In this study, we examine dune deposits as potential archives of fire history within the SE Queensland dune fields, because these landforms are abundant within the interior and along the coastlines of Australia (Lees, 2006; Hesse, 2016) and many parts of the world (Lancaster et al., 2016).

SE Queensland dune field vegetation

The SE Queensland dune fields (aka the Great Sandy Coast) in Australia (24.4°S–27.5°S) include the three largest sand islands in the world—K'gari (Fraser Island), Minjerribah (North Stradbroke Island), and Mulgumpin (Moreton Island)—and the CSM on the mainland (Fig. 1b). These dune fields have existed since ca. 800 ka (Ellerton et al., 2020, 2023). They are composed of large parabolic dunes that contain the world's largest rainforest and unconfined aquifer on a sand island and are home to rare flora and fauna (UNESCO, 2021). Their vegetation structure follows a climax succession moving inland from the coast (Walker et al., 1981, 2010). Biozones change from coastal pioneer communities, through dry sclerophyll forest (e.g., *Eucalyptus*, *Casuarina*, and *Banksia*), to wet sclerophyll forest (e.g., satinay [*Syncarpia hillii*], *Araucaria*, and ferns), and rainforest landward, with heathlands and coastal wetlands on the western (inland) side of the dune sequences (Queensland Herbarium, 2021).

While this shift in vegetation structure and composition is inferred to be reliant on nutrient and water availability (Walker et al., 1981, 1987; Thompson, 1992; Thomas, 2003), fire plays an important role in shaping this landscape (Thompson and

Moore, 1984; Walker et al., 1987; Spencer and Baxter, 2006). For example, heathlands and dry sclerophyll forest often require frequent, low-intensity fires at a minimum spacing of 8 yr to reduce ground cover and canopy shading and incorporate nutrients into the soils (Keeley, 1995; Bowman et al., 2014; Queensland Herbarium, 2021).

Wet sclerophyll forest (composed of tall sclerophyll trees with relatively dense understory vegetation such as ferns) is characterized by less frequent fires occurring in SE Queensland at a minimum of 20 yr intervals (Queensland Herbarium, 2021). In these areas, fires are generally suppressed by the forest moisture content. Even wetter are the rainforests, or more accurately, notophyllous vine thickets, that typically avoid burning in all but the driest and most extreme conditions. Local patches of rainforest within the dune fields are associated with the low-lying dune swales that are perennially wet, and when fires penetrate, they are usually low intensity; however, these systems are extremely sensitive to fire (Collins, 2019; Queensland Herbarium, 2021).

SE Queensland dune field fire history and geomorphic response

The oldest fire record from the dune island of Minjerribah, ca. 160 km south of the CSM, has preserved fire activity for at least the last ca. 210 ka. There are documented Indigenous traditions of frequent, low-intensity burning on these dune fields (Fensham, 1997; Mulholland, 2021). The oldest archaeological site on Minjerribah is at Wallen Wallen Creek and is dated to 21 ka (Neal and Stock, 1986). Dated archaeological sites on K'gari and the CSM are much younger, with the oldest published age at ca. 5.5 ka (McNiven, 1991), but it is likely that these areas have been inhabited at least as long as Minjerribah.

More recently, Indigenous land management has been absent from the dune fields and replaced by a fire-suppression regime that dates to the expansion of the timber industry ca. AD 1870 (Hawkins, 1975; Spencer and Baxter, 2006). The consequent shift to less frequent fires is easily identified in paleoecological studies (e.g., Moss et al., 2015) and has led to the transition of wet sclerophyll forests to rainforest through local fire exclusion (Krishnan et al., 2018). It is also linked to rare, higher-intensity fire events. For example, in late AD 2020, the Fraser Island Fire burned over 50% (~870 km^2) of K'gari (Fig. 1b) and is believed to have had a devastating effect on the biota of the dune fields and may be responsible for an acceleration of dune migration (Mulholland, 2021).

Indeed, fire plays a critical role in transforming the landscape (Fig. 1c–e). It is well documented that fire may lead to the formation, acceleration, and/or erosion of dunes (Levin et al., 2012; Shumack and Hesse, 2018; Ellerton et al., 2018; Patton et al., 2022a). Ellerton et al. (2018) discovered that the most recent activation of the Carlo Blowout in the CSM was initiated by fire and posited that this was unlikely to be a onetime occurrence. As was discussed in Patton et al. (2022a), fire is one of the primary factors creating the necessary conditions to destabilize steep dune hillslopes. We found that the burned sections of the 2019 Freshwater Road Fire (Fig. 1e) induced dry-ravel and sheetwash (similar to sand avalanching), but these processes were limited to the youngest dunes (Fig. 1b, Supplementary Fig. 1). We hypothesized that this was due to changes in sediment transport styles associated with hillslope gradients after fire. This study aims to help elucidate the effects of fire on dune erosional and depositional processes over multimillennial periods, and how these changes may influence our interpretations of charcoal records.

Landscapes such as the SE Queensland dune fields, with high fuel loads and proximity to consistent winds, are prone to wildfires (Filion, 1984; Thompson and Moore, 1984; Srivastava et al., 2012; Shumack et al., 2017; Ellerton et al., 2018); however, dune environments are rarely targeted for paleofire reconstruction. This is most likely because they are regarded as too ephemeral or present difficulties for extracting reliable multimillennial environmental records. There are few bogs in the CSM, so there are no fire records documented within the immediate dunes, despite the inferred importance of fire in maintaining the local environment. This is in contrast to the other SE Queensland dune fields (i.e., K'gari and Minjerribah), which have multiple charcoal records (e.g., Donders et al., 2006; Barr et al., 2013, 2017; Moss et al., 2013; Atahan et al., 2015; Mariani et al., 2019; Schreuder et al., 2019; Kemp et al., 2021; Maxson et al., 2021) from bog, lake, and fen settings. The closest records from the CSM dune field are from the Rainbow Beach patterned fen complexes approximately 10 km northwest of the dune field (Moss, 2014; Hanson et al., 2023; Fig. 2), which provide local records to compare with records from the CSM.

METHODS

Site selection and sampling design

The CSM in SE Queensland, Australia, is positioned approximately 150 km north of Brisbane and immediately south of the sand island K'gari. The dune field has an area of 240 km^2 and is composed of large parabolic dunes with crests up to 240 m above sea level. They are composed of >98% well-sorted siliceous sands (180–250 µm) (Thompson, 1983, 1992; Tejan-Kella et al., 1990). The freely drained soils and the humid subtropical climate with its warm, wet summers and mild, dry winters (mean annual precipitation = 1500 mm) (Peel et al., 2007; BOM, 2019) promote podzolization. Sediments are retained within interdune and footslope positions due to the lack of fluvial and eolian erosion following stabilization by vegetation (Patton et al., 2022a). The land-surface stability coupled with high porosity and permeability lead to the unabated development of giant podzols (Thompson, 1981). Changes in dune-form age correspond with systematic changes in soil and vegetation development. The dune field has been extensively dated (Tejan-Kella et al., 1990; Walker et al., 2018; Ellerton, et al., 2020, 2023; Patton et al., 2022b) and mapped (Ward, 2006; Patton et al., 2019).

Most dunes initiate near the coastline from disturbances such as sea-level rise, storms, and/or fires (Levin, 2011; Patton et al., 2022b). Their path inland is maintained by the nearly limitless sediment supply from the longshore-drift system (Boyd et al., 2008) and consistent SE winds (Coaldrake, 1962) until they are ultimately stabilized by vegetation (Levin, 2011). The timing of dune stabilization is penecontemporaneous with the initiation of dune sediment erosion and deposition (i.e., the transition from eolian to colluvial processes) (Patton et al., 2022b). These processes have been occurring for at least 800 ka, resulting in one of the oldest and most complex coastal dune sequences in the world (Ellerton et al., 2020, 2023).

In this study, we sampled depositional wedges at the base of four closely adjacent Holocene parabolic dunes with emplacement (stabilization) ages of 0.44 ± 0.10 ka, 2.14 ± 0.27 ka, 4.89 ± 0.45 ka, and 9.82 ± 0.98 ka, hereafter referred to as the 0.5 ka, 2 ka, 5 ka, and 10 ka dunes, respectively (Fig. 2b). The age of each dune was determined by optically stimulated luminescence (OSL) dating from dune crest positions, representing each of the four major Holocene dune activation/stabilization phases (Patton et al., 2019, 2022b; Ellerton et al., 2020; Supplementary Fig. 2). Sample sites were chosen from depositional settings at the base of the lee-side slipface of each dune (Fig. 2b). All sampled soil pits have a similar upslope source area (a planar hillslope length of <70 m to the dune crest) on a north-facing dune slipface (Fig. 2c and d) and are located in "dry" sclerophyll forest with similar vegetation types and canopy cover. The dominant taxa include pink bloodwood (*Corymbia intermedia*), scribbly gum (*Eucalyptus signata*), forest-oak (*Casuarina torulosa*), black she-oak (*Casuarina littoralis*), banksia (*Banksia serrata*), and blackbutt (*Eucalyptus pilularis*) with a canopy cover between ~60% and 80%.

Each site was hand excavated to a minimum depth of 1.75 m (Fig. 2d). Additionally, we augered at the base of each pit to determine the depth of the underlying dune surface (i.e., deposit thickness), which was identified by the presence of buried horizons (Fig. 2c). This depth is inferred to represent the initiation of sediment deposition and the timing of dune stabilization (i.e., the transition from eolian to colluvial sediment transport); therefore, we utilized the OSL ages collected from dune crest to reflect the maximum basal age of dune footslope deposits (white dot in Fig. 2c). The profile face was cleaned and described using standard soil description protocols (i.e., Schoenberger et al., 2002). Descriptions included characterizing soil horizons, grain size, boundaries of horizons, rooting depths, and soil structure. All charcoal layers and bioturbation features (e.g., ant burrows, nest construction, root growth and decay, and/or evidence of tree throws) were recorded. Charcoal fragments visible on the exposure face were sampled, labeled, and saved for radiocarbon (^{14}C) analysis.

For each soil profile, sediment samples and bulk density cores were extracted (~2000 cm^3 and ~260 cm^3, respectively) at predetermined depths, with the highest sampling density near the surface. Samples were extracted contiguously across the profile face at 0.05 m intervals from 0 to 0.1 m and then at 0.1 m intervals to 1.5 m, after which intervals of 0.25 m were used. In this study, we assign the midpoint for each sample depth interval when placing them in the context of depth and time (e.g., a depth range of 0.1–0.2 m would be reported as being at 0.15 m). Bulk density was measured using the short core extraction method (Blake and Hartge, 1986), which involves driving a core into the pit face and carefully removing it with a flat-edged soil knife. All samples were collected from the bottom of the profile upward to avoid contamination. The sampling was not initially designed with a fire record in mind, and limitations created by the sampling design are discussed later.

Sediment sample preparation

All samples were dried for 48 h at 50°C. Dried samples were passed through a 2 mm stainless steel sieve to remove the coarse fraction (CF). Very little CF was present (average 0.34 ± 0.73% by mass) and only consisted of root and charcoal fragments. This is not surprising in an eolian sand deposit. Coarse charcoal particles in the CF were handpicked and saved for radiocarbon dating. The remaining fine fraction (FF) (<2 mm) soil samples were saved and labeled to be subsampled later for charcoal counting.
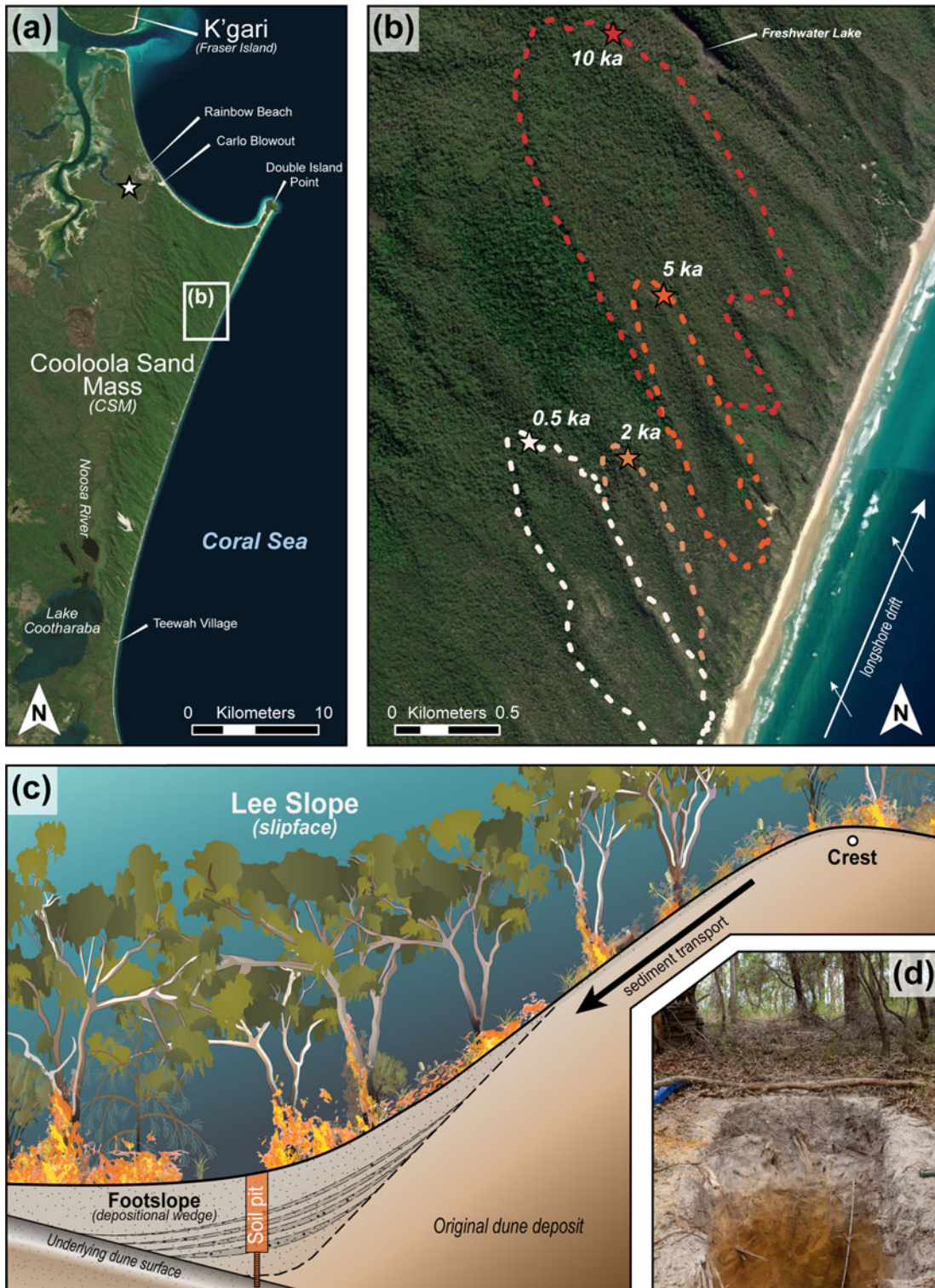
Figure 2. Site location. (a) Satellite imagery of the Cooloola Sand Mass (CSM) with areas of interest, and the Rainbow Beach patterned fen complex (white star). (b) Closeup of the four dunes used in this study (dashed lines) and locations of the depositional footslope sites (stars) found on each dune's north-facing slipface. The dunes selected in the research represent each of the four major Holocene dune activation/stabilization phases (Patton et al., 2019, 2022b; Ellerton et al., 2020; see Supplementary Fig. 2). (c) Conceptual diagram of sediment transport and deposition on a dune's slipface. Charcoal particles are produced on the dune's surface during fires (small black dots), transported down gradient, and deposited in the footslope as disseminated charcoal or charcoal layers. We hypothesize that charcoal analyzed in this study remains in stratigraphic order and is produced locally, because sediment is retained within the CSM's dune basins (Patton et al., 2022a) and charcoal particles are large (between 180 μm and 2 mm). The orange box indicates the location where soil pits were excavated to obtain a fire record for this study. A sand auger was used at the base of each pit to determine the depth of the underlying dune surface (i.e., deposit thickness). This surface is inferred to represent when sediment deposition initiated and reflects the emplacement (stabilization) ages collected from optically stimulated luminescence (OSL) samples on the dune crest (white dot). (d) Soil profile looking up to the crest on the 10 ka dune.

Bulk density

Bulk density cores retrieved from the field were oven dried for 48 h at 105°C to remove all moisture and then weighed. A 2 mm sieve was used to partition soils into CF and FF, and each fraction was weighed (m_{CF} and m_{FF}, respectively). The volume of the CF (V_{CF}) was determined for each core by dividing the m_{CF} by the density of the CF, which is assigned a constant 0.5 g/cm^3 (Eq. 1a). This density value was selected because charcoal and fine roots range between 0.4 g/cm^3 and 0.6 g/cm^3 as determined through water displacement. The V_{CF} was subtracted from the bulk density core volume (V_T), ~260 cm^3, to obtain the FF volume (V_{FF}) (Eq. 1b). Finally, FF bulk density (BD$_{FF}$) was calculated by dividing the mass by the volume (Eq. 1c) of the FF.

$$m_{CF}/0.5 = V_{CF} \qquad \text{(Eq. 1a)}$$

$$V_T - V_{CF} = V_{FF} \qquad \text{(Eq. 1b)}$$

$$m_{FF}/V_{FF} = BD_{FF} \qquad \text{(Eq. 1c)}$$

Charcoal counting

Charcoal retained in sedimentological records has been used as a proxy for fire activity and regimes (e.g., Whitlock and Larsen, 2001; Marlon et al., 2016; Hennebelle et al., 2020). Most traditional aquatic archives, such as lakes and bogs, utilize microcharcoal particles (e.g., <125 µm) that are associated with distal sources through either airborne fallout (generally ca. 1–2 km) and/or by inlet streams from the surrounding catchment area (Whitlock and Millspaugh, 1996; Whitlock and Larsen, 2001; Higuera et al. 2007). As a result, these records typically represent broad, regional fire signals that may include an amalgamation of vegetation types and biozones (Marlon et al., 2006; Vachula et al., 2018). In this study, we focus our analyses on larger macrocharcoal, which represents local (in situ) fire production originating within ca. 100 m of the dune soil profiles (e.g., Clark et al., 1998; Gavin et al., 2003; Higuera et al., 2005; Sanborn et al., 2006; Iglesias et al., 2015; Itter, et al., 2017; Leys et al., 2017; Morris et al., 2017). We analyzed charcoal >180 µm, because smaller fragments are more susceptible to eluviation processes (the vertical transport of particles through the soil profile), due to the homogenous (180–250 µm) and well-drained (600 mm/h) dune sands (Reeve et al., 1985).

FF soil samples for all depth intervals were homogenized, subsampled using a riffle splitter (~5 g), and if necessary, treated with 15 mL of 10% HCl for 24 h to remove any sesquioxide coatings on sand grains (i.e., samples collected from well-developed B horizons). Each sample was sequentially wet sieved at 355 µm, 250 µm, and 180 µm. Care was taken to not damage the charcoal fragments. Under a dissecting microscope (2×–20× magnification) all charcoal was counted (no.) in the following size classes (180–250 µm, 250–355 µm, and 355 µm–2 mm). Charcoal counts are converted to charcoal concentration by dividing the charcoal count by the subsample volume (V). The volume is calculated by using the initial subsample mass (m_i) divided by the BD$_{FF}$ from the appropriate depth interval (see Eq. 2). This was completed for all samples for each profile, and results are plotted against depth. Additionally, we compare charcoal concentrations between

each size class.

$$\text{Charcoal concentration} = \left(\frac{\text{no.}}{[m_i/BD_{FF}]}\right) = \left(\frac{\text{no.}}{[V]}\right) \qquad \text{(Eq. 2)}$$

Charcoal selection and preparation for radiocarbon (^{14}C) dating

Even in regions with homogenous geomorphology and ecology, it is necessary to acquire a large number of dates to adequately resolve fire history. To build a chronological framework for each depositional profile, we selected charcoal samples to be radiocarbon (^{14}C) dated by accelerator mass spectrometry (AMS). Our primary targets were >2-mm-diameter charcoal fragments picked directly from the profile face of known absolute depths (n = 24). We supplemented these samples with charcoal within the CF (n = 22), and although these charcoal samples have inherently higher uncertainty with regard to depth (i.e., they come from intervals of 0.05 m to 0.25 m), they provide a means to evenly distribute radiocarbon dating across all profiles.

Radiocarbon samples were dated at two laboratories, with 46 samples dated in total. Twelve samples were dated at the Waikato Radiocarbon Dating Laboratory in 2019 and 2021. A further 34 samples were dated at the Australian Nuclear Science and Technology Organisation (ANSTO) radiocarbon laboratory in 2021 and 2022 (Fink et al., 2004). At both laboratories, the charcoal samples were pretreated using the standard acid–base–acid (ABA) protocol before being combusted and graphitized (Hua et al., 2001). Sample graphite was then loaded into aluminum cathodes and measurements were determined by AMS. The results were reported in conventional radiocarbon age or percent modern carbon (pMC) (see Table 1).

Age–depth model and combining charcoal records

For all profiles, age–depth models were created using the rbacon package (Blaauw and Christen, 2011) in R (R Core Team, 2020), with the calibration data being the Southern Hemisphere calibration curve (SHCal20; Hogg et al., 2020) extended to recent time using the post-bomb atmospheric calibration curve for Southern Hemisphere zone 1–2 (Bomb22SH1-2; Hua et al., 2022). All the modeled ages were reported in calibrated years before 1950 (cal yr BP) at 95% confidence interval. Additionally, we set the surface age to 2019 (i.e., −69 cal yr BP; date of sample collection) and the basal ages to the OSL-dated dune ages collected from dune crest (Fig. 2c). We attributed the age for each sample to the midpoint of each sample depth range. Charcoal records were evaluated by plotting sample depth to charcoal concentration (particles/cm^3). We normalize for changes in sedimentation rates within and between sites by calculating charcoal accumulation rates (CHAR) expressed in units of particles/cm^2/yr (Long et al., 1998). Charcoal production can vary among sites due to local conditions (i.e., moisture content, fire intensity, and biomass); therefore, we rescaled each record to range from 0 to 1 by dividing by the maximum CHAR value (Power et al., 2008). Once normalized, records were combined and plotted against time to establish a composite master charcoal record for the Holocene dune field. For all charcoal records, CHAR peaks were identified visually.
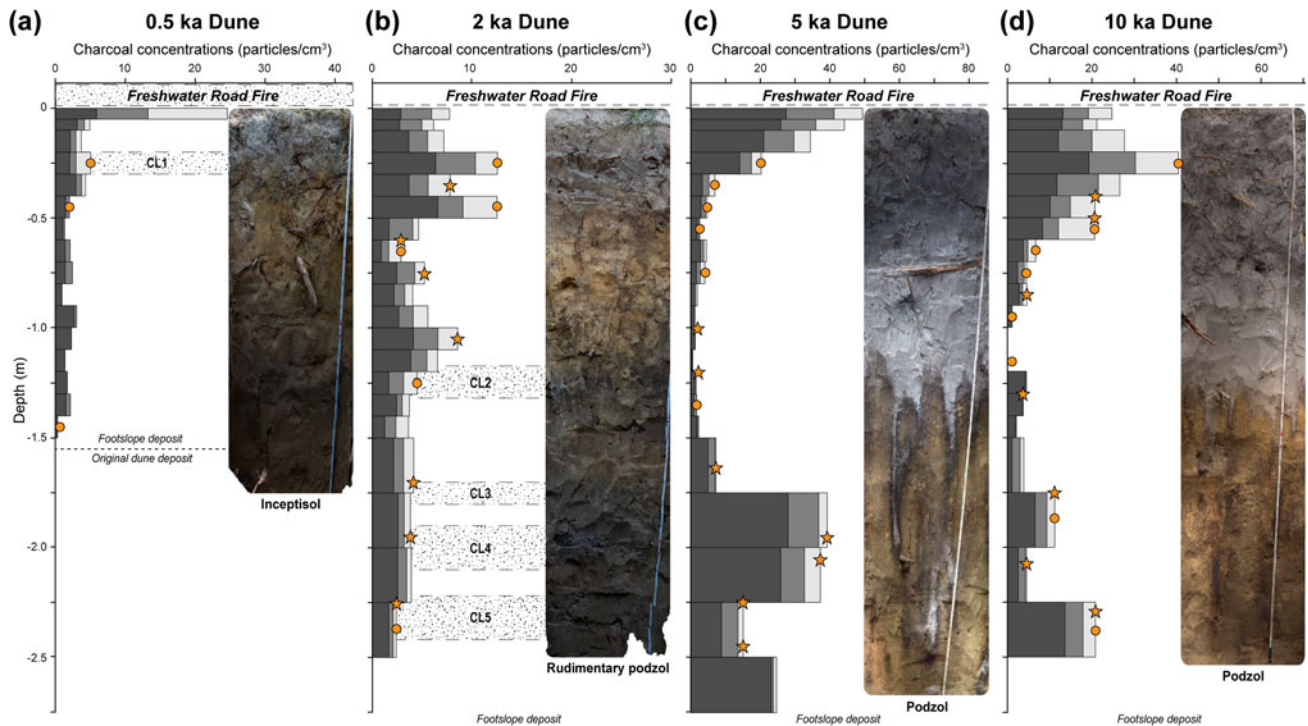
Figure 3. Charcoal concentrations for the (a) 0.5 ka, (b) 2 ka, (c) 5 ka, and (d) 10 ka dune depositional sites. For each depth interval (width of bar) charcoal was counted for size classes 180–250 μm (dark gray), 250–355 μm (gray), and 355 μm–2 mm (light gray). Charcoal layers identified in the profile face are indicated by a band of black dots and labeled (CL1–CL5). Samples collected for radiocarbon analysis are indicated with an orange star or an orange circle depending on whether they were collected at a discrete depth or from a sample depth interval, respectively. Charcoal layers only occur on the two youngest dunes and were incorporated in multiple sample intervals due to predetermined sampled depths. Note, the Freshwater Road Fire severely burned and deposited fresh charcoal at the surface of all sites (dashed lines labeled "Freshwater Road Fire") after pit excavation and sample collection, but only produced a 0.1 m charcoal-rich dry-ravel deposit at the 0.5 ka site. As a result, no charcoal concentrations were recorded for this interval. For more information on each soil profile see Supplementary Figs. 4–8.

Our results were compared with published charcoal records from a nearby patterned fen complex (Hanson et al., 2023) and two lake records with similar forest types and, presumably, similar fire histories (Donders et al., 2006; Mariani et al., 2019) (white stars in Fig. 1b, Supplementary Fig. 3). Additionally, we compared the results with Mooney et al.'s (2011) and Williams et al.'s (2015) subtropical high-pressure belt (25°S–45°S) record of biomass burning. The purpose of this cross-site comparison was to assess whether our master charcoal record depicted reasonable local trends and/or evidence of broad regional fire-regime changes as compared with those derived from more traditional (aquatic) archives.

RESULTS

Field observations and soil characterization

Soil profiles were excavated to a maximum depth of 2.75 m and were classified from youngest to oldest as an inceptisol, rudimentary podzol, podzol, and podzol (Fig. 3). As expected, all soils have uniform grain-size distributions concentrated between 180 μm and 250 μm. The younger profiles from the 0.5 ka and 2 ka dunes have minimal pedogenic development, and charcoal is dispersed throughout the profile; however, distinct charcoal layers (CL) are observed. The 0.5 ka profile had one layer (CL1: 0.2–0.3 m), and no charcoal was observed >1.5 m. All sediment below 1.6 m was classified as primary dune sediment due to its lack of soil development and absence of organic material. The 2 ka profile had four charcoal layers near the base (CL2:

1.20–1.30 m; CL3: 1.70–1.80 m; CL4: 1.90–2.10 m; and CL5: 2.20–2.40 m). In contrast, the oldest profiles from the 5 ka and 10 ka dunes have distinct transitions between the pedogenic horizons, with the exception of the boundary between the A and E horizons, which is diffuse. Charcoal was disseminated throughout the profile, with elevated concentrations at the base and near the surface. Additionally, several months after pit excavations the Freshwater Road Fire (Fig. 1b and e) burned all site locations. The fire removed vegetation and deposited charcoal at the surface, but only induced a ~0.1 m sand ravel deposit on the 0.5 ka dune footslope (Fig. 3a, Supplementary Fig. 1). This deposit was not included in our charcoal analyses and is only utilized as a point of discussion.

For all sites, root growth and decay are the most prevalent forms of postdepositional mixing. This activity is greatest at the surface and rapidly decreases with depth, such that most roots are confined within the A horizon (<0.5 m depth). Unexpectedly, we observed little evidence of other common forms of bioturbation (i.e., ant mounds, rodent burrows, tree throws, and/or nest construction). This is in stark contrast to the upslope, eroding positions at the CSM, where all these processes are commonly observed and where we visually estimated up to 3 ant colonies/m² along the hillslope surface.

Charcoal concentrations

Charcoal at all sites was well preserved (black, angular, and opaque). Concentrations were consistent across all the sites, and all size classes depicted similar trends with depth (Fig. 3,

Table 1. All ages used to produce age–depth models in this study are from woody macrocharcoal (^{14}C) and primary dune sands (optically stimulated luminescence [OSL]) are reported in years relative to 1950 (Fig. 4).[a]

Sample no.	Lab ID[b]	Depth (m)	OSL ages (ka ± 1σ)	Conventional ^{14}C ages (yr BP ± 1σ)	Calibrated ages (95% confidence interval) (cal yr BP)	Modeled calibrated ages (95% confidence interval) (cal yr BP)
0.5 ka Dune						
—	Surface	0	—	—	−69[c]	−69 (−66 to −72)
1	OZAF02	0.20–0.30	—	102.61 ± 0.32[d]	−5 (0 to −9)	11 (49 to −4)
2	OZAF03	0.40–0.50	—	170 ± 25	116 (278 to −3)	59 (102–17)
3	OZAF04	1.40–1.50	—	220 ± 25	192 (298 to −4)	266 (300–178)
—	USU-2283[e]	1.60[f]	0.44 ± 0.10	—	—	292 (344–205)
2 ka Dune						
—	Surface	0	—	—	−69[c]	−69 (−66 to −72)
4	OZAE96	0.20–0.30	—	335 ± 25	389 (448–300)	398 (463–299)
5	Wk-52211	0.35	—	718 ± 18	628 (666–565)	575 (598–512)
6	OZAE97	0.40–0.50	—	625 ± 25	604 (635–535)	608 (633–555)
7	Wk-52212	0.60	—	640 ± 19	608 (636–545)	644 (673–613)
8	OZAE98	0.60–0.70	—	980 ± 30	852 (924–771)	680 (712–639)
9	Wk-52213	0.75	—	882 ± 21	745 (793–683)	703 (751–680)
10	Wk-52214	1.05	—	960 ± 19	852 (907–768)	780 (814–745)
11	Wk-50298[g]	1.20–1.30	—	1017 ± 26	857 (930–798)	820 (855–791)
12	OZAE99	1.70	—	955 ± 30	834 (917–740)	895 (928–864)
13	Wk-50299	1.95	—	1023 ± 24	859 (955–800)	945 (981–908)
14	OZAF01	2.25	—	1080 ± 25	944 (1047–908)	1031 (1082–957)
15	Wk-50300	2.35–2.41	—	1166 ± 24	1013 (1062–960)	1060 (1169–1002)
—	USU-3021[h]	5.10[f]	2.14 ± 0.27	—	—	2373 (2679–2109)
5 ka Dune						
—	Surface	0	—	—	−69[c]	−69 (−66 to −72)
16	OZAE83	0.2–0.3	—	270 ± 25	285 (322 to −4)	354 (456–184)
17	OZAE84	0.3–0.4	—	1350 ± 25	1225 (1285–1177)	1203 (1282–1085)
18	OZAE85	0.4–0.5	—	1815 ± 25	1662 (1747–1590)	1425 (1661–1282)
19	OZAE86	0.5–0.6	—	1535 ± 20	1367 (1411–1314)	1502 (1811–1361)
20	Wk-50296	0.7–0.8	—	2397 ± 26	2381 (2671–2179)	2056 (2211–1732)
21	OZAE87	1.0	—	2290 ± 25	2225 (2341–2143)	2253 (2343–2148)
22	OZAE88	1.20	—	2410 ± 25	2401 (2684–2332)	2406 (2489–2336)
23	OZAE89	1.30–1.40	—	2585 ± 25	2626 (2753–2493)	2523 (2605–2410)
24	OZAE90	1.65	—	2665 ± 25	2752 (2845–2718)	2717 (2767–2570)
25	OZAE92	1.75–2.00	—	2695 ± 25	2769 (2849–2737)	2783 (2854–2741)
26	OZAE91	1.90	—	2795 ± 25	2848 (2946–2772)	2796 (2868–2760)
27	OZAE93	2.10	—	2630 ± 30	2734 (2777–2516)	2858 (2979–2805)
28	Wk-50297	2.25	—	2624 ± 25	2733 (2767–2518)	2932 (3076–2840)
29	OZAE94	2.45	—	2760 ± 30	2818 (2920–2754)	3059 (3246–2922)
—	USU-2284[e]	5.30[f]	4.89 ± 0.45	—	—	5716 (6328–5197)

(Continued)

Table 1. (*Continued.*)

Sample no.	Lab ID[b]	Depth (m)	OSL ages (ka ± 1σ)	Conventional ^{14}C ages (yr BP ± 1σ)	Calibrated ages (95% confidence interval) (cal yr BP)	Modeled calibrated ages (95% confidence interval) (cal yr BP)
10 ka Dune						
—	Surface	0	—	—	−69[c]	−69 (−66 to −72)
30	OZZ591	0.20–0.30	—	560 ± 25	—	—
31	OZZ592	0.20–0.30	—	365 ± 35	392 (487–309)	421 (493–308)
32	OZAE76	0.40	—	1905 ± 25	1792 (1875–1725)	1752 (1824–1611)
33	OZAE77	0.50	—	1955 ± 25	1858 (1928–1749)	1856 (1924–1761)
34	OZZ594	0.50–0.60	—	1950 ± 35	1852 (1985–1746)	1905 (1998–1834)
35	OZAE78	0.60–0.70	—	2275 ± 25	2231 (2337–2140)	2174 (2271–2105)
36	OZZ596	0.70–0.80	—	2160 ± 35	2087 (2298–2003)	2284 (2524–2225)
37	Wk-50293	0.85	—	3534 ± 24	3768 (3871–3652)	2823 (3699–2445)
38	OZAE79	0.90–1.00	—	2860 ± 25	2926 (3060–2848)	3008 (3960–2849)
39	OZZ597	1.10–1.20	—	5040 ± 70	5743 (5900–5600)	4982 (5358–4285)
40	OZAE80	1.30	—	4815 ± 25	5522 (5590–5334)	5381 (5570–5074)
41	Wk-50294	1.75	—	5305 ± 26	6062 (6183–5934)	5997 (6152–5922)
42	OZAE81	1.75–2.00	—	5485 ± 30	6240 (6308–6125)	6123 (6235–6011)
43	OZAE82	2.07	—	5495 ± 30	6246 (6385–6128)	6277 (6385–6197)
44	Wk-50295	2.30	—	5648 ± 26	6375 (6483–6305)	6455 (6602–6359)
45	OZZ598	2.25–2.50	—	5880 ± 35	6659 (6778–6502)	6553 (6688–6442)
46	OZZ599	2.90	—	5995 ± 35	6788 (6895–6670)	7124 (7393–6834)
—	USU-2285[e]	4.50[f]	9.82 ± 0.98	—	—	10,215 (11,196–9414)

[a]Age calibration was performed using the Southern Hemisphere calibration curve (SHCal20; Hogg et al., 2020) extended to recent time using the post-bomb atmospheric calibration curve for Southern Hemisphere zone 1–2 (Bomb22SH1-2; Hua et al., 2022), and modeled ages were produced using rbacon (Blaauw and Christen, 2011) in R (R Core Team, 2020).
[b]Lab numbers beginning with Wk, OZ, and USU were analyzed at the Waikato Radiocarbon Dating Laboratory, Australian Nuclear Science and Technology Organisation (ANSTO), and Utah State University Luminescence Laboratory, respectively.
[c]Surface date in cal yr BP.
[d]A modern sample, whose measured ^{14}C content was reported in percent modern carbon (pMC) instead of conventional ^{14}C age.
[e]Originally published in Ellerton et al. (2020) in years relative to AD 2018.
[f]Depth indicates the maximum depth of each footslope deposit (depositional wedge). These depths are assigned a basal age that represents timing of dune stabilization and are obtained from OSL ages collected from dune crests.
[g]Originally published in Patton et al. (2022a) in years relative to AD 1950.
[h]Originally published in Patton et al. (2022b) in years relative to AD 2020.

Supplementary Fig. 4). The 180–250 μm size class contributes approximately half of the cumulative charcoal concentrations for each depth interval, whereas the larger size classes (250–355 μm and 355 μm–2 mm) each contributed about a quarter of the cumulative charcoal concentrations. For this reason, we simplify our results by only reporting aggregate charcoal concentrations hereafter. Combined charcoal concentrations from all size classes (i.e., combined charcoal counts from 180 μm to 2 mm) are measured from 0 to 49.4 particles/cm^3, with the highest values found near the surface. Out of the 78 sampled depth intervals, only three samples lacked charcoal (not including samples at depths >160 cm from the 0.5 ka dune, which constitutes the original dune deposit). The average charcoal concentrations for each profile generally increased with dune age from 3.9 ± 5.7, through 5.8 ± 2.8, and 14.5 ± 16.6, to 13.9 ± 11.6 particles/cm^3.

Radiocarbon (^{14}C) analysis and age–depth modeling

Radiocarbon results from 46 charcoal particles produced ages ranging from 0.01 to 7.125 cal ka BP (Table 1). We analyzed 12, 14, and 17 radiocarbon samples from the 2 ka, 5 ka, and 10 ka dunes, respectively. The 0.5 ka dune had few radiocarbon targets and only yielded three ages. Due to our sampling strategy, 52% of the total dates are younger than 2 cal ka BP. We observe consistent trends with depth, with only four age reversals (> ±2σ) (Fig. 4). The ages of the sampled intervals represent a range of ages owing to the contiguous sampling design (see Supplementary Table 1); however, we find samples from the same depth interval within sites yield similar ages (e.g., samples 33 and 34; samples 44 and 45 in the 10 ka dune). Sedimentation rates are the highest where charcoal layers are present (i.e., the entire 0.5 ka dune and below 1.20 m on the 2 ka dune). In general, rates decrease moving up the excavated profiles toward the surface.

CHAR records

Charcoal concentrations are converted into CHAR using accumulation rates derived from the age–depth models. We find that all CHAR values ranged from 0 to 11.6 particles/cm^2/yr, and each

record shows distinct peaks in CHAR that are detected among sites and size classes (Fig. 5, Supplementary Fig. 4). The 0.5 ka dune has one peak at the surface, whereas the 2 ka dune has a peak between ca. 1.1 and 0.4 cal ka BP. The 5 ka dune record has two peaks. The most recent occurred within the last 0.3 ka and the earlier peak at ca. 3.4–2.6 cal ka BP. The 10 ka dune has four peaks at ca. 6.7–5.3 cal ka BP, peaks between ca. 3.0–2.6 and 2.2–1.6 cal ka BP, and the most recent started ca. 0.5 cal ka BP. When the individual records are combined into a composite master record, we observe five peaks occurring between ca. <0.3, 1.1–0.4, 2.2–1.6, 3.4–2.6, and 6.7–5.3 cal ka BP (vertical orange bars in Fig. 5e) regardless of inclusion or exclusion of CHAR values associated with episodic sediment transport (white line or black area in Fig. 5e, respectively). In general, CHAR peaks increase in frequency after ca. 3.4 cal ka BP, with the highest values in the last century.

Not all CHAR peaks register as visible charcoal layers in the soil profiles. Charcoal layers (CL1–CL5) are only observed within the two youngest sites (Fig. 3a and b). These differences are due to the relatively coarse and contiguous sampling intervals and not all charcoal used for radiocarbon dating being from discrete depths. This caused charcoal layers to be incorporated in multiple samples (Fig. 3), including those with low charcoal concentrations, resulting in a smoothed CHAR record.

DISCUSSION

Charcoal preservation within dune footslope deposits

Previous studies have successfully used charcoal records from paleosols in blowouts, deflation basins, and swales to understand dune activity with respect to changes in climate and fire regimes (e.g., Filion, 1984; Seppälä, 1995; Käyhkö et al., 1999; Mann et al., 2002; Arbogast and Packman, 2004; Carcaillet et al., 2006; Matthews and Seppälä, 2014). This study represents the first attempt to systematically target dune footslopes (depositional wedges in front of dune slipfaces) to reconstruct a fire record. We propose that dune footslopes are appropriate targets for paleofire reconstruction. Footslopes at the CSM are depositional systems that produce sequences of locally derived sediments. Most or all inorganic sediments produced on the adjacent hillslope (dune front avalanche face) are inferred to be deposited and preserved with little disruption or mixing. Short-term hiatuses are likely present, but field observations demonstrate only minor physical postdepositional mixing of particles >180 μm. These are limited to the near surface through root growth and decay. The lack of physical mixing is supported by intact and distinct soil horizons, consistent charcoal concentrations among size classes, and consistent increases in age with depth. Only four age reversals are observed in our records, and they likely record minor reworking in upbuilding soil A horizons (Almond and Tonkin, 1999; Fig. 4).

Fires are common in the dune field (e.g., Mulholland, 2021), and charcoal is present throughout the profile of the colluvial footslope deposits. As the sites are located within a ca. 2 km radius from each other, the similarity of the records is expected, and indeed necessary, if these types of sites are to be used to produce reliable fire histories. As depicted in the 0.5 ka dune (Fig. 3a), there is no evidence of macrocharcoal (>180 μm) found within the original dune deposit (>1.6 m depth), which suggests charcoal in these depositional profiles must be incorporated after dune emplacement (stabilization). In fact, our previous studies indicated no evidence of charcoal in the primary eolian

deposits from our sampled Holocene dunes (Ellerton et al., 2020; Köhler et al., 2021; Patton et al., 2022b). The absence of charcoal from primary dune sands within the CSM likely reflects the limited area for fire to initiate in the upwind direction (i.e., the Coral Sea) and the challenge for fire to penetrate into active dunes due to their limited woody fuel loads (Fig. 2b).

Our local records indicate wildfires that occurred within the CSM's dry sclerophyll forest impacted most dune slopes. Perhaps the best evidence for the preservation of paleofire records is that CHAR peaks are traceable between the different profiles (Fig. 5), and the trends are consistent regardless of charcoal size classes (Supplementary Fig. 4). For instance, the 0.5 ka, 5 ka, and 10 ka deposits identified the same ca. <0.3 ka CHAR peak, the 5 ka and 10 ka footslope share the CHAR peak at ca. 3 cal ka BP, and all sites had fresh charcoal deposited on their surfaces from the Freshwater Road Fire (Fig. 3).

An important observation is that we observe minor variability between our records. Fires can be extremely localized and confined to specific sections of the dune field due to the direction of fire propagation or naturally occurring firebreaks (i.e., low-lying swales with high humidity and/or barren sand patches). Indeed, this may explain the differences between our depositional records, especially when episodic sediment transport dominates (within the first ca. 1.5 ka of sediment deposition). However, it could be the result of our sampling design, which lacks the necessary resolution to capture all changes in charcoal production and/or events (Fig. 5). For instance, the 2 ka dune depicts one CHAR peak that incorporates four charcoal layers (CL2–CL5) from ca. 1.1 to 0.4 cal ka BP but did not register at the older sites despite being positioned windward of those sites. This is inferred to be the result of the coarse sample size, which incorporated both periods of low and high biomass burning within the same sample, thereby obscuring potential CHAR peaks (see sample locations: dots in Fig. 5c and d).

Alternatively, the discrepancies could reflect variations in charcoal production or preservation between sites. Cohen-Ofri et al. (2006) demonstrated that oxidizing conditions like those found within the CSM (<5 pH) may degrade charcoal structure, thereby lowering charcoal preservation potential. The charcoal found within our depositional footslopes are large, woody, and structurally strong (slightly hard to hard consistency). Moreover, we find that average charcoal concentrations between the oldest and youngest sites are nearly four times greater despite having been exposed to acidic conditions longer. Although our coarse sampling design prohibited us from addressing this concern, we believe that chemical degradation of charcoal into fragments smaller than our analyses (180 μm–2 mm) is minor and thus does not affect our interpretations. Nevertheless, future studies should consider the preservation potential of charcoal in acidic soil conditions when constructing a fire history.

Sedimentation inferences from the age–depth models

In our previous work, we characterized the first phase of dune hillslope development as occurring through episodic sediment transport (dry-ravel and sheetwash) induced by disturbances such as fire on the steep initial dune gradients (Patton et al., 2022a). These perturbations resulted in rapid topographic adjustments (increased footslope sedimentation rates). We discovered that once dune gradients are lowered below their angle of repose (0.65 m/m or 33°), which occurs ca. 1 ka after dune stabilization, a second phase of gradual hillslope evolution with steady and
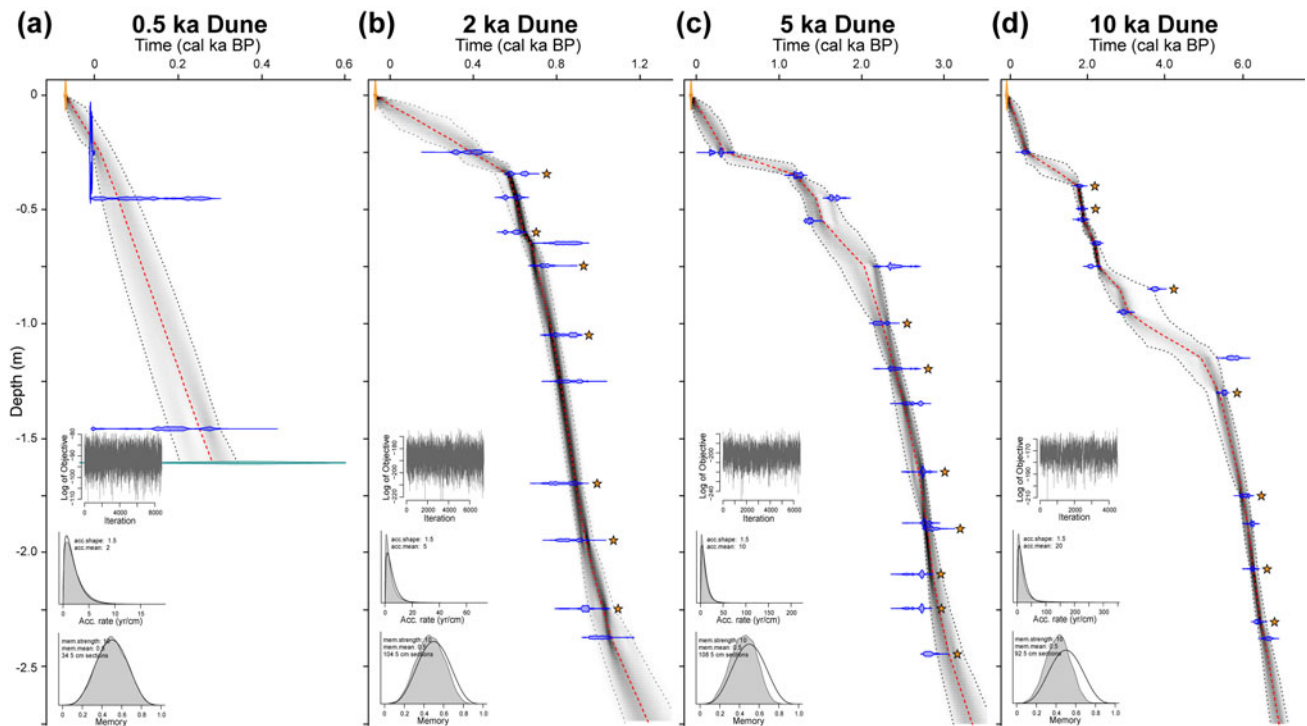
Figure 4. Bayesian age–depth models generated for the (a) 0.5 ka, (b) 2 ka, (c) 5 ka, and (d) 10 ka dune depositional sites. For each site, we set the age of the surface (0 m) to the date of pit excavation (vertical orange marker), and the basal age to the optically stimulated luminescence (OSL)-dated dune age collected from dune crest. All cal. ages are obtained through radiocarbon (^{14}C) dating of charcoal fragments using the Southern Hemisphere calibration curve (SHCal20; Hogg et al., 2020) extended to the recent time using the Post-bomb Atmospheric calibration curve for Southern Hemisphere zone 1-2 (Bomb22SH1-2; Hua et al., 2022). Graphs were produced using 'rbacon' (Blaauw and Christen, 2011) in R (R Core Team 2020). The calibrated year probability distributions estimates are shown as blue and aqua markers for ^{14}C and OSL ages, respectively. The red dashed line bounded by the gray dotted lines represents the age–depth model best fit and the 95% confidence intervals, respectively. Note, the y-axis only extends to 2.75 m, which covers all sample intervals, and does not include the complete age–depth model that extends to the base of each deposit (original dune deposits or onlapped topography). Additionally, samples collected from discrete depths are labeled with an orange star.

continuous sediment transport (soil creep processes) begins. Indeed, the geochronological and sedimentological data in this study support these assertions.

The age–depth models from the four deposits yield similar trends of increasing age with depth (Fig. 4) and indicate no substantial break in sedimentation or evidence of erosion (truncated horizons), supporting the idea that these dune positions are consistently depositional (Patton et al., 2022a). Additionally, we find that sedimentation rates decrease with dune age, which is to be expected due to the "Sadler effect" (Sadler, 1981), which may lead to biases in sedimentological records if not accounted for (Vachula et al., 2022). We attempt to account for this effect by averaging the median sediment rate in 100 yr intervals for each footslope deposit and find that sedimentation rates decrease with age from 0.34 ± 0.17, through 0.16 ± 0.13 and 0.05 ± 0.05, to 0.03 ± 0.02 cm/yr.

When plotting our sedimentation rates for each sample interval as a function of time since dune stabilization, we find a distinct transition at ca. 1.5 ka (Fig. 6a). Interestingly, the abrupt shift in sedimentation rates coincides with the presence or absence of charcoal layers found within the excavated sections of the footslope deposits. For example, the ca. 1.5 ka transition occurs at 0.35 m depth on the 2 ka dune, which is above the boundary between charcoal preserved in distinct layers and charcoal dispersed throughout (Fig. 3b).

We find a substantial difference in the average sedimentation rate between sampled intervals before and after the 1.5 ka transition (i.e., sections associated with either charcoal layers or

disseminated charcoal) with mean values of 0.57 ± 0.13 and 0.10 ± 0.07 cm/yr, respectively (Fig. 6b). Our results support that differences in sedimentation rates are associated with the transition from the dominance of episodic to continuous sediment transport on the dune hillslopes (Patton et al., 2022a; Fig. 6). Moreover, these findings highlight the idea that the change from presence to absence of charcoal layers reflects a geomorphic process (the transition from dominance of episodic to continuous sediment transport).

In fact, the observed 0.1 m deposit during the Freshwater Road Fire of 2019 (Fig. 3a, Supplementary Fig. 1) onto the footslope of the 0.5 ka dune is consistent with the sedimentation rates during the first phase of sedimentation when charcoal layers are present. For sclerophyll forests, such as those found on the CSM, fires are estimated to occur at ca. 20 yr intervals (Keith, 2004). Assuming the Freshwater Road Fire is representative of past fires and that the multimillennial fire frequency–magnitude relationship is appropriate, we would expect a fire to deposit ∼10 cm of sediment on average within each 20 yr interval (equivalent to a fire-induced sedimentation rate of 0.5 cm/yr). This estimate is consistent with the sedimentation rates observed in the 0.5 ka and 2 ka deposits, and reflects the contribution associated with episodic sediment transport. Sediment will also actively move downslope even without the perturbation of fire through continuous soil transport processes (e.g., granular relaxation, rain splash, and biogenic soil creep), which we estimated to be an order of magnitude lower (Patton et al., 2022a).
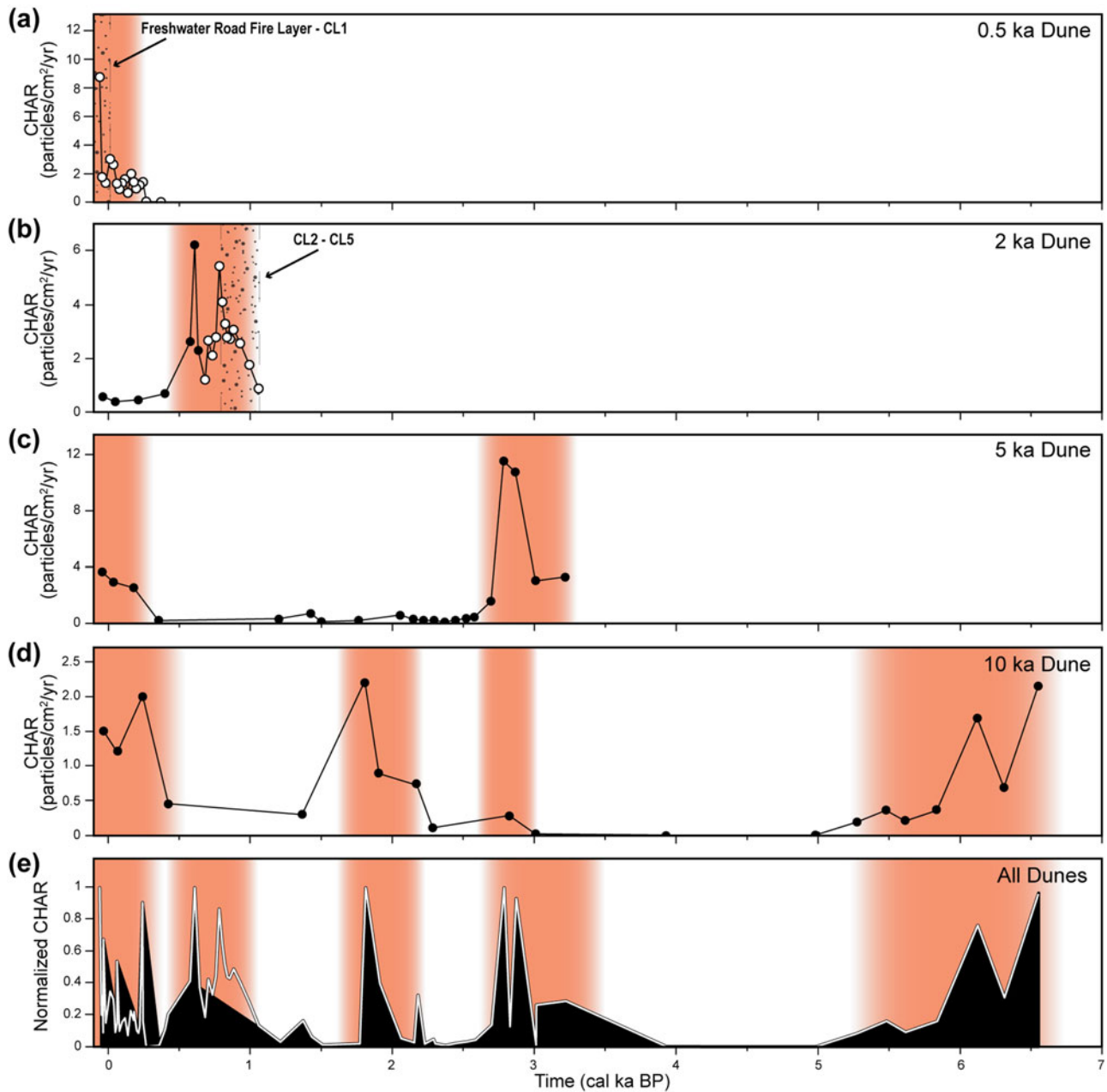
Figure 5. Charcoal accumulation rates (CHAR) and the inferred timing of increased fire activity (peaks are vertical orange areas) for the (a) 0.5 ka, (b) 2 ka, (c) 5 ka, and (d) 10 ka dune depositional sites. Locations for all samples are marked with dots, such that white dots indicate episodic sediment transport (sheetwash or dry-ravel) associated with the first 1.5 ka of sediment deposition, while black dots indicate slow and continuous sediment transport (soil creep). Charcoal layers (CL) found in profile faces (Fig. 3) are indicated by a band of black dots and labeled (CL1–CL5). For more information on CHAR for each size class and the locations for all charcoal layers, see Supplementary Fig. 4. (e) A composite master charcoal record was derived from all four sites by dividing each record by its maximum CHAR value and then plotting the normalized CHAR with time. The white line represents a record composed of all CHAR values (n = 77), whereas the black area represents samples that only experienced continuous sediment transport (n = 48).

Implications of charcoal layers in dune deposits

Rates of sedimentation and the presence or absence of charcoal layers (CL) are intimately coupled with geomorphic and ecological processes and must be considered when generating fire records. In the section, we discuss whether CHAR peaks and/or charcoal layers in pit faces represent fire-based events (Figs. 5 and 3, respectively) and provide plausible mechanisms for their presence within our dune deposits.

It is not straightforward to determine whether CHAR peaks or charcoal layers represent individual wildfires. For CHAR peaks, sampling intervals could span more than one fire event, and even where sampling intervals are narrow, these intervals may reflect several centuries of accumulation. This is particularly true for fire records that lack a strong chronological framework (limited age constraints) and/or have charcoal samples with large inbuilt ages, both of which can make interpretations difficult. Although we are confident in our age–depth modeling due
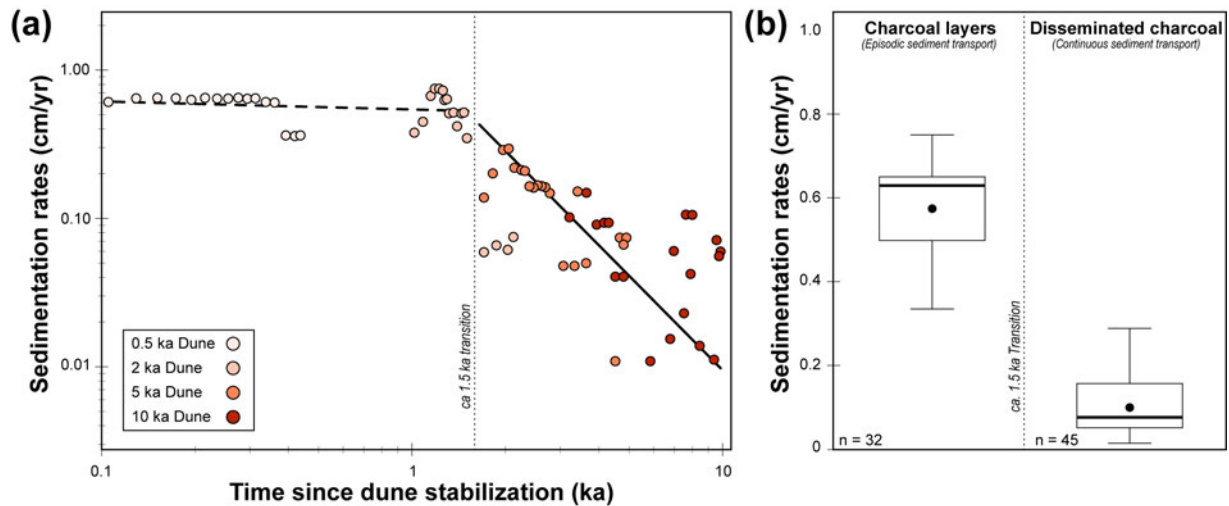
Figure 6. (a) A log-log plot of the median sedimentation rate for all sampled intervals (dots) from each footslope deposit as a function of time since dune stabilization. Sedimentation rates are initially high (dashed line) then abruptly decrease after ca. 1.5 ka (solid line). (b) Box and whisker plots for sedimentation rates before and after this transition. Boxes are the interquartile range, with the whiskers representing maximum and minimum values. The black dot is the mean, and the horizonal black line represents the median. We hypothesize that the shift in sedimentation rates reflects the transition from episodic (dry-ravel and sheetwash) to continuous sediment transport styles (soil creep) and is associated with the presence or absence of charcoal in layers, respectively. Note that the separation between these two sedimentation rates occurs ca. 1.5 ka after dune emplacement, which is comparable to the findings in Patton et al. (2022a), where we estimated ca. 1 ka for this transition to occur.

to our large quantity of radiocarbon and OSL dates (n = 50) and small inbuilt ages (ca. 10 yr; sample 2 in Table 1), there are always uncertainties in these analyses (e.g., Whitlock and Larsen, 2001). Therefore, it is inappropriate to claim elevated CHAR values represent single fire events, such as those found in sections where sedimentation rates are low (e.g., peak at ca. 2.2–1.6 cal ka BP in Fig. 5d). We propose that individual fire events cannot be identified from CHAR peaks alone, but rather should be used to indicate phases of increased biomass burning (Long et al., 1998; Remy et al., 2018).

Charcoal layers, however, are likely an event-based deposit (Mathews and Seppälä, 2014) (i.e., CL1–CL5 in Fig. 5a and b and Supplementary Figs. 5 and 6). As discussed earlier, layers are only formed before ca. 1.5 ka after dune stabilization, when dune hillslope gradients are above their angle of repose and perturbations such as fires can induce episodic sediment transport near the dune crest. The short (<70 m) and steep (0.65 m/m or 33°) hillslopes promote the rapid delivery of sediments to their subjacent footslopes (e.g., as we observed following the Freshwater Road Fire; Supplementary Fig. 1). These observations indicate that long-term storage of charcoal on hillslopes during this phase is unlikely; therefore, we propose that charcoal layers in pit faces are associated with individual fire events.

An important caveat is that not all fires on oversteepened slopes induce episodic sediment transport, and those that do, do not induce sediment transport evenly across the landscape. To initiate dry-ravel and sheetwash (similar to a sand avalanche), soil cohesion needs to be decreased (Reid and Dunne, 1996; Roering and Gerber, 2005). This can occur through the removal of organic matter, reduction of water content and roots, or production of hydrophobic surface soils (Bridge and Ross, 1983; Doerr et al., 2000; Shakesby and Doerr, 2006). These disturbances to the hillslope are dependent on the severity of the fire and are unlikely to be consistent between events (DeBano, 1981). This was demonstrated during the Freshwater Road Fire, where

episodic sediment transport styles were not observed evenly across all slipfaces near or at the angle of repose. It is reasonable to assume that only the largest and hottest fires are likely to be represented as woody charcoal layers across multiple sampling locations, whereas layers that occur at only one sample site are likely to reflect local fire conditions.

From our dune footslope sites, we find that there is a clear geomorphic and ecological record preserved within the stratigraphy. We observe three stratigraphic deposits within our sites: (1) sand lacking charcoal; (2) sand with charcoal in layers; and (3) sand with dispersed charcoal. We hypothesize that these records directly relate to the vegetation structure and composition and the dominant active sediment transport style (Fig. 7). While dunes are active or stabilizing, woody charcoal–producing fire is rare. In this phase, sand is exposed with only minor patches of vegetation that are composed of grasses and small shrubs (Levin, 2011). The ability of fire to spread is limited, and the lack of woody biomass hinders the production of charcoal, specifically in the larger size classes utilized in this study. Consequently, the sediment delivered from the dune crest to the footslopes through slipface avalanching and granular flows is barren of macrocharcoal (Fig. 7a).

Once the dunes are stabilized, dry sclerophyll forest begins to develop through vegetation succession (Walker et al., 1981); hence fire becomes more prevalent and woody charcoal production increases. We estimate this succession in the CSM to occur ca. 0.3 ka after dune stabilization due to the presence of ~1-m-diameter *Corymbia intermedia* found on the 0.5 ka dune upslope positions that are estimated to be ca. 175–350 yr old (Ngugi et al., 2020; Supplementary Fig. 1a). Charcoal produced on the slopes is rapidly transported down gradient through dry-ravel and sheetwash, forming charcoal layers (Fig. 7b). However, episodic sediment transport only occurs while the gradients are above the angle of repose of the dry unconsolidated dune sands. Once gradients are lowered below this threshold, only continuous sediment processes such as granular relaxation or soil creep
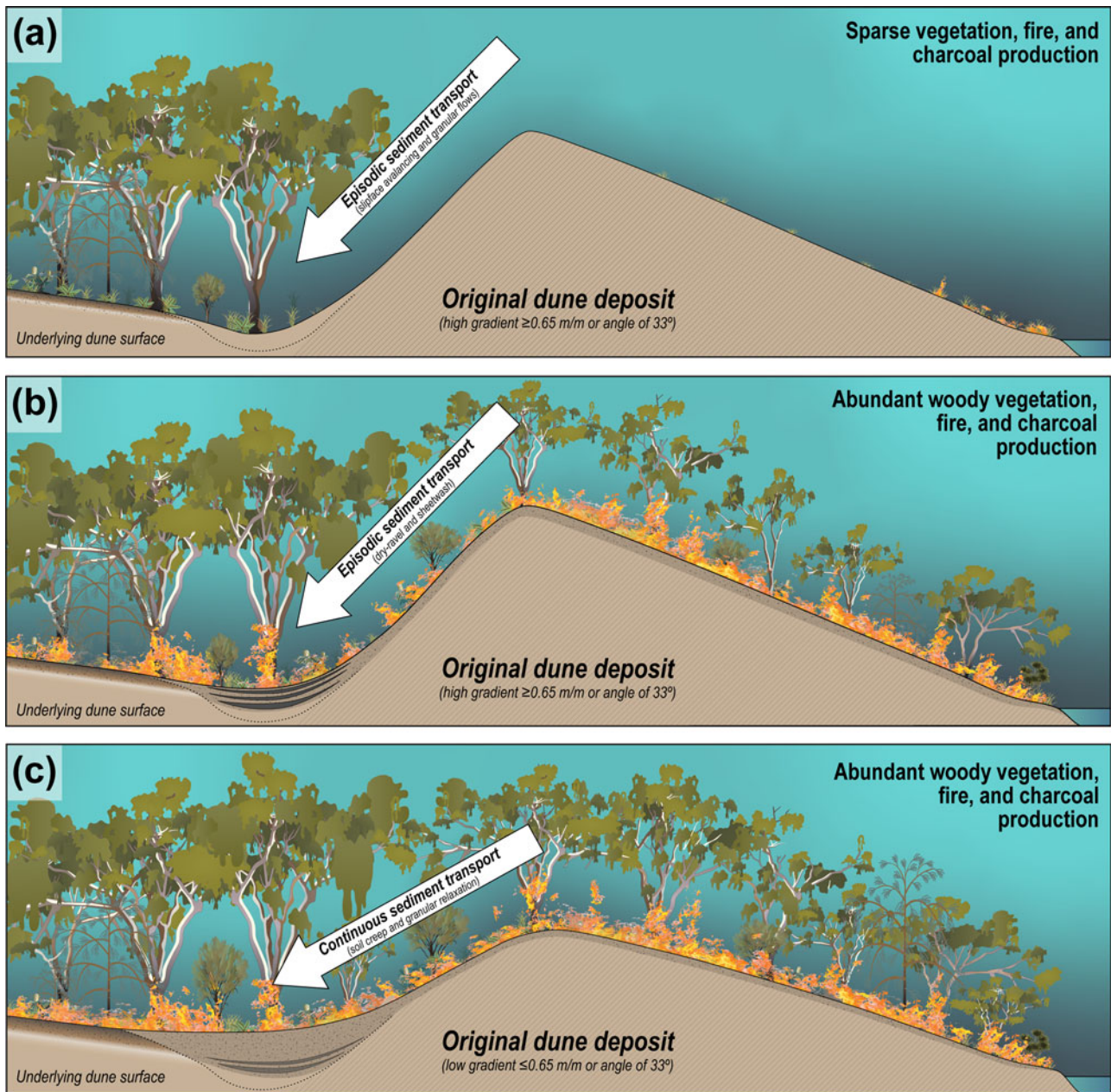
Figure 7. Conceptual diagram of progressive vegetation succession, fire activity, charcoal production, and stratigraphic deposit for an (a) active dune with steep gradients, (b) recently emplaced (stabilized) dune with steep gradients, and (c) emplaced dune with shallow gradients. When dunes are active, vegetation is sparse and fires are assumed to be infrequent and unproductive (a). As woody vegetation such as *Eucalyptus* spp. or *Corymbia* spp. becomes established, charcoal production increases (black dots). Charcoal can either be deposited in the footslope positions as layers (black lines in b) or disseminated throughout the profile (gray areas in b and c). The presence or absence of charcoal layers is the result of episodic sediment transport processes (e.g., dry-ravel and sheetwash) and elevated charcoal production on dune gradients that are above the sand's angle of repose (b). The absence of layers but the presence of disseminated charcoal implies slow and continuous sediment transport (i.e., granular relaxation and biogenic soil creep) (c).

prevail (Roering et al., 1999; BenDror and Goren, 2018; Patton et al., 2022a). This transition is estimated to occur ca. 1.5 ka after dune stabilization, as indicated by the significant decrease in the sedimentation rates beginning at 0.35 m in the 2 ka dune (Figs. 4b and 6). Despite the potential for fire and charcoal production to remain high during this phase, the absence of episodic sediment transport results in only the preservation of disseminated charcoal, with higher and lower CHAR rates representing increasing or decreasing biomass burning, respectively (Fig. 7c).

Comparison of CSM's dune paleofire records with records from the wider region

CHAR values from charcoal layers provide useful insights on sediment transport styles and local fire events; however, these layers should be used cautiously when developing fire records due to their spatial variability within a small area. Therefore, to compare our findings with other local and regional records, we utilize the composite master charcoal record from CHAR values linked to consistent sedimentation styles and rates (disseminated charcoal) (black area in Figs. 5e and 8a), as these deposits should reflect

general trends of biomass burning without conflating geomorphic and ecological processes.

Our composite master charcoal record indicates three major periods of fire activity in the past ca. 7 cal ka BP that reflect those records derived from lake and swamp deposits in the SE Queensland dune fields and in the wider subtropical high-pressure belt of eastern Australia (24°S–45°S) (Fig. 8). We observe that the earliest peak at ca. 6.7–5.3 cal ka BP corresponds with charcoal records from Minjerribah (Fig. 8d) and a compilation of sites across the nontropical east coast of Australia (Fig. 8e). The Lake Allom record on K'gari (Fig. 8c) registers elevated CHAR values at ca. 7 cal ka BP before a hiatus from ca. 6.5 to 5.4 cal ka BP (Donders et al., 2006). In the wider region, a downward trend in CHAR is observed during this period (Mooney et al., 2011). The only exception is the ca. 4.5 ka charcoal event at the Rainbow Beach patterned fen complex (Moss, 2014; Hanson et al., 2023), where a local fire close to the patterned fen is the likely source of the elevated CHAR (Fig. 8b). This period of reduced burning was followed by an upswing in fire activity with a large CHAR peak from ca. 3.4 to 2.6 cal ka BP, with a smaller peak in CHAR at ca. 2.2–1.6 cal ka BP that is observed in all local and regional records. These late Holocene events are only observed in SE Queensland. At ca. 1.1–0.4 cal ka BP, there is a gradual increase in burning and CHAR peaks at the CSM, at the Rainbow Beach patterned fen complex, and Lake Allom. Although this peak is absent from the macrocharcoal record from Swallow Lagoon on Minjerribah (Fig. 8b), it is present within its microcharcoal record (Mariani et al., 2019). All records show a marked increase in CHAR over the last few centuries between ca. 5 and 0.2 cal ka BP. In summary, the CSM's dune footslope fire records are compatible with those from traditional fire records found within SE Queensland.

Causes of the high CHAR periods

As noted in Figure 8, the charcoal records in the SE Queensland dune fields can be divided into three major periods. Period 1, before ca. 5.3 cal ka BP, shows elevated charcoal indicating increased local burning, while Period 2 has little evidence of fires between ca. 5.3 and 3.4 cal ka BP. This matches records obtained from K'gari and Minjerribah (Donders et al., 2006; Atahan et al., 2015; Schreuder et al., 2019; Mariani et al., 2019) and across the subtropical high-pressure belt (Mooney et al., 2011; Williams et al., 2015). The disruption in biomass burning coincides with increases in total rainfall with lower relative variability associated with less frequent El Niño events during period 2 (Barr et al., 2019; Fig. 9b–d). An alternative explanation for the transition may be the result of the termination of the postglacial transgression (Lewis et al., 2008). Before ca. 5.5 cal ka BP, the coastline would have extended significantly seaward from its modern position, which would result in more dune field (land) being seaward of all footslope deposits and increasing the likelihood of fire reaching the sample sites. These hypotheses are not mutually exclusive and indeed likely are the result of both scenarios.

Period 3 shows that fire frequency has gradually increased over the last ca. 3.4 cal ka BP (Fig. 8). This increase in CHAR is observed within many SE Queensland records. K'gari records indicate that after ca. 4 cal ka BP, fire activity progressively increased (e.g., Donders et al., 2006; Atahan et al., 2015; Schreuder et al., 2019). The elevated fire activity was ascribed to increased occupation and amplified Indigenous burning practices

(Schreuder et al., 2019); however, this is difficult to evaluate due to the limited archaeological data available. Alternatively, the increased fire activity is hypothesized to relate to changes in the hydrological cycle primarily through the intensification of the El Niño–Southern Oscillation (ENSO) (Shulmeister and Lees, 1995; Moy et al., 2002; Donders et al., 2006; Conroy et al., 2008; Barr et al., 2019) with minor shifts in vegetation type (Donders et al., 2007; Mariani et al., 2019). Again, it is likely that both intensification of human usage and ENSO affected the fire records but may also reflect an artifact of increased sampling frequency in these sediment sections.

At the end of period 3, there is an increase in biomass burning that is widely observed in records across Australia and the world (e.g., Kershaw et al., 2002; Power et al., 2008; Mooney et al., 2011; Williams et al., 2015). This elevated biomass burning in Australia is inferred to be a direct result of climate change (Power et al., 2008; Mooney et al., 2011) exacerbated by European fire suppression (Hanson et al., 2022; Mariani et al., 2022).

Climate variability drives vegetation communities and thereby available fuel load and fire frequency in the dry sclerophyll forest of subtropical Australia (Mariani et al., 2019). In years with higher water availability, fuel loads increase but fires are suppressed by the moisture content. Dry years enable fires to occur, but the reduced fuel loads make them less intense and frequent. In both scenarios, stable wet or dry climates result in relatively reduced fire risk. In contrast, when interannual climate varies strongly, a condition the SE Queensland dune fields have experienced in the Late Holocene (Barr et al., 2019), fuel loads are able to build up in wet years and cure in the subsequent dry ones, resulting in increased fire activity and intensity (Bradstock, 2010).

Geomorphic and ecological controls on dune paleofire records

Biomass burning can be primarily ascribed to climate-mediated vegetation changes; however, it is important to consider how geomorphic processes may influence vegetation, fire activity, and charcoal deposition (Fig. 7). Across the SE Queensland dune field, CHAR records closely reflect progressive vegetation succession associated with phases of dune activation and emplacement (stabilization) (Fig. 9, Supplementary Fig. 9). We observe that CHAR peaks are inversely related to the timing of major phases of dune emplacement and likely reflect the inability of fire to penetrate through active dune fields. The presence of charcoal in the dune footslope deposits is partially controlled by the local composition of vegetation in the windward direction (SE) on the dune hillslopes (Fig. 7). The first evidence of charcoal occurs directly after the first phases of dune activation at 8.5 ± 1.0 ka during the postglacial transgression (Ellerton et al, 2020; Patton et al., 2022b) (Fig. 9, Supplementary Fig. 9). As sea level rose, dunes were active off the coast and migrated inland (vegetation-free landscape) for years to centuries before stabilizing (e.g., Levin, 2011; Houser et al., 2015; Levin et al., 2017). While the dunes are active, they act as a natural fire break that hinders the encroachment of fire spreading from the windward direction (Fig. 7a). Not until the emergence of woody vegetation such as *Eucalyptus* spp. or *Corymbia* spp. do woody charcoal–bearing fires occur (Fig. 7b and c). These findings matched those found in the Nebraska Sand Hills in the United States, where fire frequency and pollen abundance were inversely related to eolian activity (Schmieder et al., 2013).
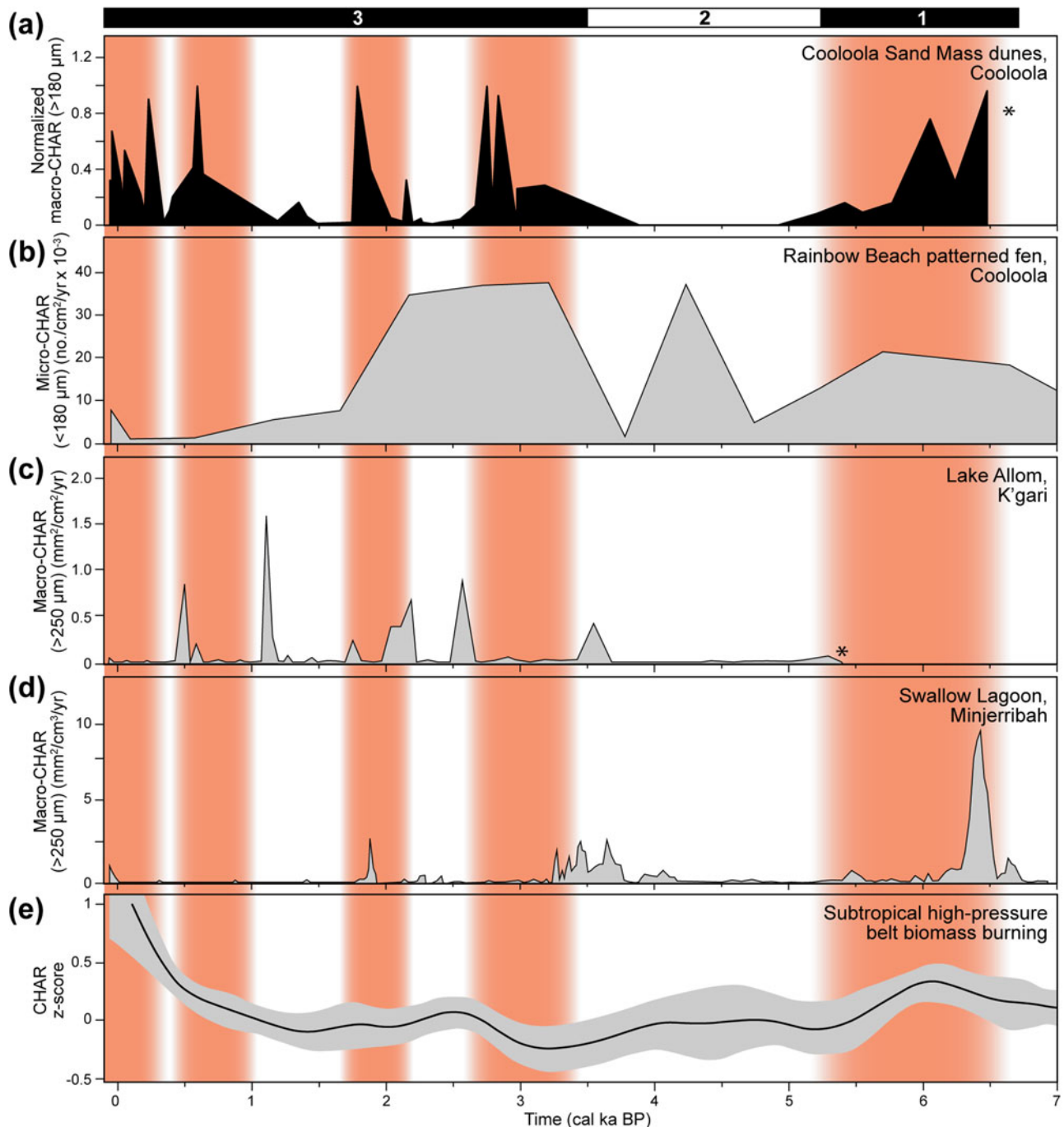
Figure 8. (a) Master charcoal record derived from only slow and continuous sediment transport for all sites in this study with increases in biomass burning (vertical orange bars) over three proposed periods of fire activity (black and white bar). Our data are compared with other (b) local (Hanson et al., 2023) and (c and d) regional sites (Donders et al., 2006; Mariani et al., 2019), as well as (e) a compilation of records from the subtropical high-pressure belt in eastern Australia (125 sites) (Mooney et al., 2011). Locations of local and regional records are indicated in Fig. 1 as white stars. The fire records from the Cooloola Sand Mass (CSM) sites are compatible with those from traditional fire records within SE Queensland (i.e., peats, bogs, and lakes). An asterisk (*) indicates the lack of data.

An important caution is that dune activation does not influence fire records equally. Although, dune activation will result in some form of disruption to the vegetation, only the largest dunes will significantly impact the charcoal records. For example, only large active dunes that extend several kilometers inland would pose a substantial barrier for fires. Once vegetated with grasses and shrubs, these dunes become highly flammable

ignition sources. These same processes will occur on small dunes but to a lesser extent and under localized conditions.

Recommendations and future applications

Wildfires are prevalent across the world, but fire histories are limited to where wetland sediment records are relatively abundant
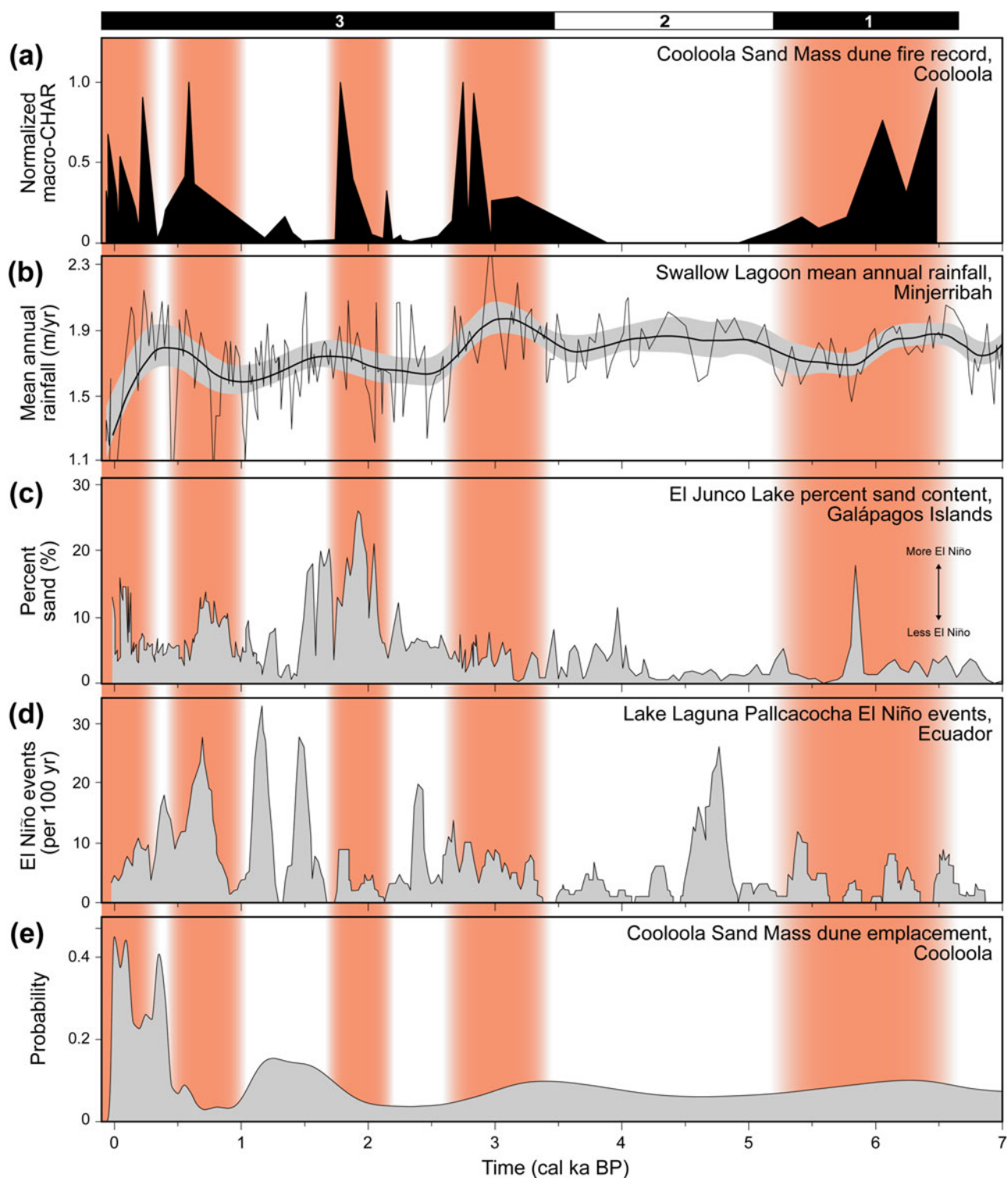
Figure 9. (a) Master charcoal record derived from only slow and continuous sediment transport for all sites in this study (black area). We compare our results with (b) the Swallow Lagoon precipitation record (Barr et al., 2019) and (c) the El Junco Lake in the Galápagos Islands and (d) the Lake Laguna Pallcacocha in southern Ecuador records of past El Niño event frequency (Moy et al., 2002; Conroy et al., 2008). Finally, we compare the (e) probability density function for the timing of dune emplacement at the Cooloola Sand Mass (CSM) (Patton et al., 2022b).

(Fig. 10). Our study identifies dune footslope deposits as a previously unrecognized record that can help explain past fire regimes and/or provide evidence for how ecosystems, such as those found in Australia, are adapted or not adapted to fire (Fig. 10). Although, this study is based on large, coastal dunes in SE Queensland, we believe these outcomes are not unique to this area. Other similar high-quality records should be present in smaller and older dunes across the world, and we encourage further exploration and methodological development in these archives. A clear path of future research would be to target
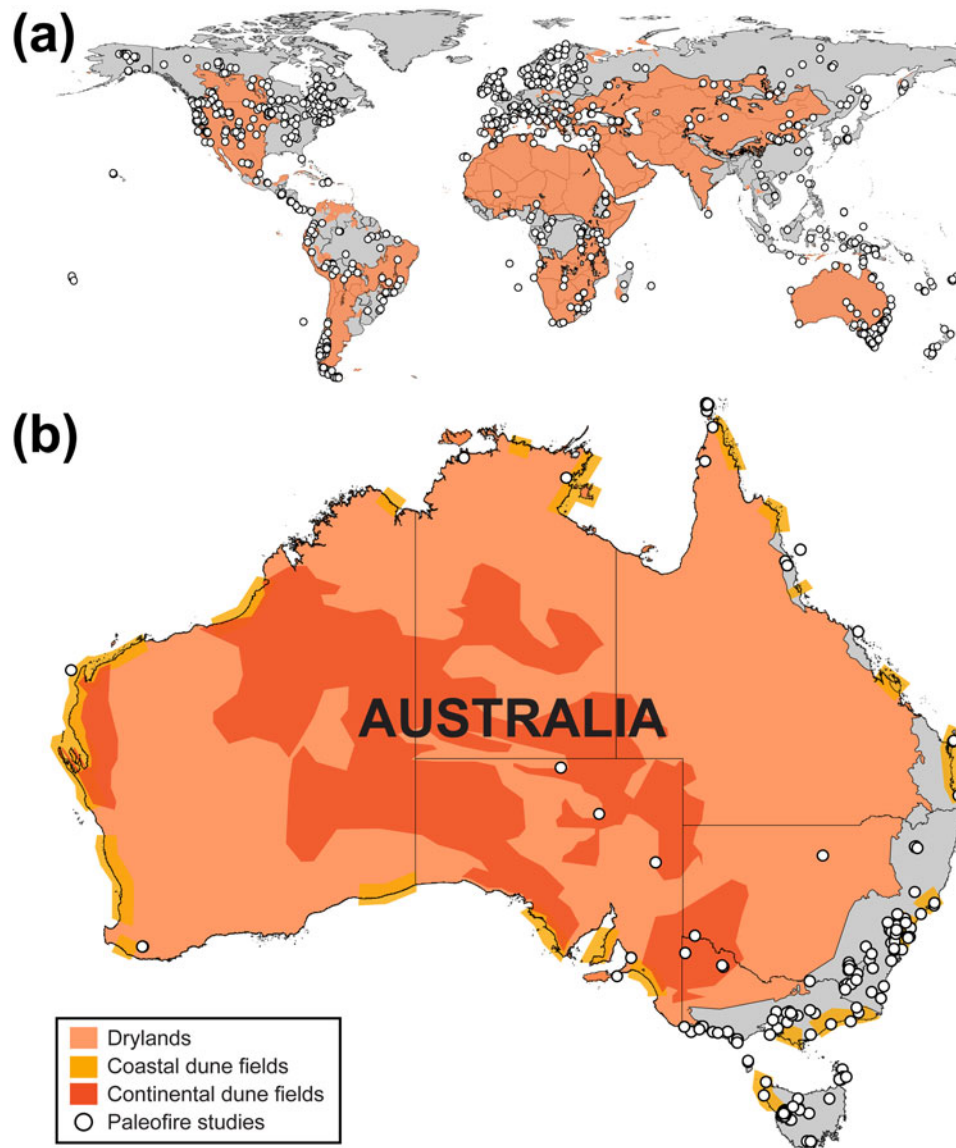
Figure 10. (a) World dryland distribution (orange areas) (Sorensen, 2007) and published paleofire records (white dots) from the Global Paleofire Database (Harrison et al., 2022). (b) Closeup view of Australia and the general locations of coastal (yellow) and continental (orange) dunes (Lees, 2006; Hesse, 2016). Note the abundant land area in Australia and the world that is both covered in drylands and lacking fire histories. Dune depositional deposits present an opportunity to expand fire records from wetland areas into dryland regions, which to this point have been underrepresented in paleofire studies.

underrepresented regions such as drylands, where fire records are sparse. We highlight Mediterranean regions, California, and the southwestern United States, northern and southern Africa, and central China as likely high-value targets for this work (Fig. 10a). We provide suggestions on selecting sites and sampling strategies in future studies.

As developed in this study, a network of depositional sites to construct a fire record is encouraged but not necessary. A singular site of significant antiquity coupled with a higher-resolution sampling design can provide useful and continuous local fire records. However, we suggest targeting multiple older, Pleistocene-aged dunes that cover similar time periods. This will increase record length, improve comparison between sites, and reduce biases created by oversampling younger depth intervals. Moreover, it is critical to avoid dunes that have experienced recent reactivations, as their foot-slopes are prone to hiatuses and large shifts in sediment rates. These

data sets are necessary if we are attempting to understand broadscale shifts in fire regimes over glacial–interglacial cycles.

The largest improvement to this study is to undertake a higher-resolution, consistent sampling regime, like those used on lake sediment cores (e.g., 1 cm samples collected every 2 or 5 cm). This would ensure that CHAR peaks are not obscured, ^{14}C dates are collected at discrete depths, and age–depth models are representative of each site. Furthermore, it is important to select samples for fire reconstruction from intervals with consistent sedimentation rates and styles to decrease the risk of conflating geomorphic and ecological processes. As our work highlights, the first ca. 1.5 ka of sediment deposition is dynamic, and fire records may reflect extremely localized and stochastic signals (i.e., CL2–CL5 in Fig. 5b). After this point, sedimentation rates are reduced, and the dominant signal is inferred to represent more regional trends in biomass burning. Determining the timing

of this transition is critical, as this shift from episodic to continuous sediment transport is unique to each site and relates to the physical properties of the dune sands (Patton et al., 2022b). However, the transition can be easily recognized from the change-over from charcoal layers to dispersed charcoal. While charcoal layers (CL) do not record regional trends in fire activity, they should not be discounted or ignored. Their presence in deposits elucidates processes and relative rates and indicates local fire events. Moreover, this simple identification of charcoal layers in deposits can rapidly aid in site selection, without the immediate need for ^{14}C dating and age–depth modeling.

CONCLUSIONS

The largest spatial gaps in fire records come from semiarid and arid regions, which lack the aquatic records favorable for preserving charcoal (Leys et al., 2018; Harrison et al., 2022). However, dunes are abundant in these regions (Thomas and Wiggs, 2008) and may provide a useful target for paleofire reconstruction. In this study, we demonstrate the potential of dune footslope deposits as an archive of multimillennial fire records. We establish that the sclerophyll forest on the stabilized dunes in the CSM in Australia have burned repeatedly and produced abundant charcoal over a ca. 7 ka period.

The large charcoal size classes (180–250 µm, 250–355 µm, and 355 µm–2 mm) selected to represent the presence of local fires show consistent concentrations and accumulation rates (CHAR) with depth from all our sites. These findings support the hypothesis that footslope deposits have experienced limited postdepositional mixing and that sites contain intact and reliable stratigraphic records of fire activity. We find that the dune depositional stratigraphy reflects one of three distinct phases with respect to charcoal production and preservation:

1. **Absent to sparse charcoal:** As dunes are active or becoming stabilized, there is insufficient vegetation to allow fires to fully develop and penetrate.
2. **Charcoal layers:** Once the dunes are stabilized by the colonization of vegetation, charcoal production increases and episodic sediment transport dominates. This results in the creation of charcoal layers associated with individual major fire events.
3. **Dispersed charcoal:** After dune slopes drop below their angle of repose and transition to slow and continuous sediment transport (at ca. 1.5 ka), charcoal continues to be deposited but is dispersed throughout the profile. During these times, individual fires cannot be identified but relative biomass burning can be inferred.

We observe five CHAR peaks found within the three major periods that are traceable between dune footslope records. In general, fire becomes more abundant after ca. 3.4 cal ka BP, which is seen in other records from lakes and swamps in the SE Queensland dune fields (i.e., K'gari's Lake Allom, CSM's patterned fen complex, and Minjerribah's Swallow Lagoon). Our findings correlate with earlier inferences that the shift in fire activity is partially due to changes in the hydrological cycle through the ENSO intensification and its impact on fuel loads. This increase may also reflect intensification of fire usage by the Indigenous people. However, we also propose an alternative hypothesis: the mechanism causing fire variability is through vegetation changes in the dune field driven by dune activity itself.

The consistent trends of increasing age with depth and relatively minor uncertainty make these depositional footslope positions ideal targets for paleofire reconstruction. We propose that other dune deposits will yield comparable findings and that these records can expand fire histories from areas where fire is a rare event (wetlands/lakes) into the parts of the landscape where fire may be an important or the dominant ecological process. Furthermore, this method opens many new regions for paleofire studies and can give new insights on fire frequency and intensity in regions globally (Fig. 10).

Data availability statement. All data necessary to generate results for this study are available in the article and Supplementary Information. The Black Summers fire extent (DAWE, 2020), world dryland distribution information (Sorensen, 2007), and the global paleofire data (Harrison et al., 2022) used in this study were downloaded from www.environment.gov.au/fed/catalog/search/resource/details.page?uuid=%7B9ACDCB09-0364-4FE8-9459-2A56C792C743%7D%20, and http://datadownload.unep-wcmc.org/datasets, and www.paleofire.org/index.php, respectively.

Supplementary material. The supplementary material for this article can be found at https://doi.org/10.1017/qua.2023.14

REFERENCES

Almond, P.C., Tonkin, P.J., 1999. Pedogenesis by upbuilding in an extreme leaching and weathering environment, and slow loess accretion, south Westland, New Zealand. *Geoderma* **92**(1–2), 1–36.

Arbogast, A.F., Packman, S.C., 2004. Middle-Holocene mobilization of aeolian sand in western upper Michigan and the potential relationship with climate and fire. *The Holocene* **14**, 464–471.

Archibald, S., Lehmann, C.E., Gómez-Dans, J.L., Bradstock, R.A., 2013. Defining pyromes and global syndromes of fire regimes. *Proceedings of the National Academy of Sciences USA* **110**, 6442–6447.

Atahan, P., Heijnis, H., Dodson, J., Grice, K., Le Métayer, P., Taffs, K., Hembrow, S., Woltering, M., Zawadzki, A., 2015. Pollen, biomarker and stable isotope evidence of late Quaternary environmental change at Lake McKenzie, southeast Queensland. *Journal of Paleolimnology* **53**, 139–156.

Barr, C., Tibby, J., Marshall, J.C., McGregor, G.B., Moss, P.T., Halverson, G.P., Fluin, J., 2013. Combining monitoring, models and palaeolimnology to assess ecosystem response to environmental change at monthly to millennial timescales: the stability of Blue Lake, North Stradbroke Island, Australia. *Freshwater Biology* **58**, 1614–1630.

Barr, C., Tibby, J., Moss, P.T., Halverson, G.P., Marshall, J.C., McGregor, G.B., Stirling, E., 2017. A 25,000-year record of environmental change from Welsby Lagoon, North Stradbroke Island, in the Australian subtropics. *Quaternary International* **449**, 106–118.

Barr, C., Tibby, J., Leng, M.J., Tyler, J.J., Henderson, A.C.G., Overpeck, J.T., Simpson, G.L., *et al.*, 2019. Holocene El Niño–Southern Oscillation variability reflected in subtropical Australian precipitation. *Scientific Reports* **11**, 7634.

BenDror, E., Goren, L., 2018. Controls over sediment flux along soil-mantled hillslopes: insights from granular dynamics simulations. *Journal of Geophysical Research: Earth Surface* **123**, 924–944.

Blaauw, M., Christen, J.A., 2011. Flexible paleoclimate age-depth models using an autoregressive gamma process. *Bayesian Analysis* **6**, 457–474.

Blake, G.R., Hartge, K.H., 1986. Bulk density. In: Klute, A. (Ed.), *Methods of Soil Analysis*. Part 1, *Physical and Mineralogical Methods* 5.1. 2nd ed. American Society of Agronomy–Soil Science Society of America, Madison, WI, pp. 363–375.

[BOM] Bureau of Meteorology, 2019. Climate Data Online. Australian Government, Bureau of Meteorology (accessed April 8, 2019). www.bom.gov.au/climate/data/index.shtml.

Bowman, D.M., 1998. The impact of Aboriginal landscape burning on the Australian biota. *New Phytologist* **140**, 385–410.

Bowman, D.M., Murphy, B.P., Neyland, D.L., Williamson, G.J., Prior, L.D., 2014. Abrupt fire regime change may cause landscape-wide loss of mature obligate seeder forests. *Global Change Biology* **20**, 1008–1015.

Bowman, D.M.J.S., Balch, J.K., Artaxo, P., Bond, W.J., Carlson, J.M., Cochrane, M.A., D'Antonio, C.M., et al., 2009. Fire in the Earth system. *Science* **324**, 481–484.

Boyd, R., Ruming, K., Goodwin, I., Sandstrom, M., Schröder-Adams, C., 2008. Highstand transport of coastal sand to the deep ocean: a case study from Fraser Island, southeast Australia. *Geology* **36**, 15–18.

Bradstock, R.A., 2010. A biogeographic model of fire regimes in Australia: current and future implications. *Global Ecology and Biogeography* **19**, 145–158.

Bradstock, R.A., Williams, J.E., Gill, A.M. (Eds.), 2002. *Flammable Australia: The Fire Regimes and Biodiversity of a Continent*. Cambridge University Press, Cambridge.

Bridge, B.J., Ross, P.J., 1983. Water erosion in vegetated sand dunes at Cooloola, south-east Queensland. *Zeitschrift für Geomorphologie, Supplementband* **45**, 227–244.

Bridgman, H., Timms, B.V., 2012. Australia, climate and lakes. In: Bengtsson, L., Herschy, R.W., Fairbridge, R.W. (Eds.), *Encyclopedia of Lakes and Reservoirs*. Springer, Dordrecht, Netherlands, pp. 73–80.

Canadell, J.G., Meyer, C.P., Cook, G.D., Dowdy, A., Briggs, P.R., Knauer, J., Pepler, A., Haverd, V., 2021. Multi-decadal increase of forest burned area in Australia is linked to climate change. *Nature Communications* **12**, 1–11.

Carcaillet, C., Richard, P.J., Asnong, H., Capece, L., Bergeron, Y., 2006. Fire and soil erosion history in East Canadian boreal and temperate forests. *Quaternary Science Reviews* **25**, 1489–1500.

Chang, J.C., Woodward, C., Shulmeister, J., 2014. A snapshot of the limnology of eastern Australian water bodies spanning the tropics to Tasmania: the land-use, climate, limnology nexus. *Marine and Freshwater Research* **65**, 872–883.

Chang, J.C., Woodward, C., Shulmeister, J., 2017. Reconstructing terrestrial temperatures in the Australian sub-tropics and tropics: a chironomid based transfer function approach. *Quaternary International* **449**, 136–148.

Clark, J.S., Lynch, J., Stocks, B.J., Goldammer, J.G., 1998. Relationships between charcoal particles in air and sediments in west-central Siberia. *The Holocene* **8**, 19–29.

Clarkson, C., Jacobs, Z., Marwick, B., Fullagar, R., Wallis, L., Smith, M., Roberts, R.G., et al., 2017. Human occupation of northern Australia by 65,000 years ago. *Nature* **547**, 306–310.

Coaldrake, J.E., 1962. The coastal sand dunes of southern Queensland. *Proceedings of the Royal Society of Queensland* **72**, 101–16.

Cohen-Ofri, I., Weiner, L., Boaretto, E., Mintz, G., Weiner, S., 2006. Modern and fossil charcoal: aspects of structure and diagenesis. *Journal of Archaeological Science* **33**, 428–439.

Collins, L., 2019. Eucalypt forests dominated by epicormic resprouters are resilient to repeated canopy fires. *Journal of Ecology* **108**, 310–324.

Conroy, J.L., Overpeck, J.T., Cole, J.E., Shanahan, T.M. Steinitz-Kannan, M., 2008. Holocene changes in eastern tropical Pacific climate inferred from a Galápagos lake sediment record. *Quaternary Science Reviews* **27**, 1166–1180.

[DAWE] Department of Agriculture, Water and the Environment, 2020. *Preliminary Analysis for Environmental Analysis—2019/20 Fires*. Department of Agriculture, Water and the Environment, Canberra (accessed May 15, 2022). www.environment.gov.au/fed/catalog/search/resource/details.page?uuid=%7B9ACDCB09-0364-4FE8-9459-2A56C792C743%7D.

DeBano, L.F., 1981. *Water Repellent Soils: A State-of-the-Art*. Vol. 46. U.S. Department of Agriculture, Forest Service, Pacific Southwest Forest and Range Experiment Station, Berkeley.

Doerr, S.H., Shakesby, R.A., Walsh, R., 2000. Soil water repellency: its causes, characteristics and hydro-geomorphological significance. *Earth-Science Reviews* **51**(1–4), 33–65.

Donders, T.H., Wagner, F., Visscher, H., 2006. Late Pleistocene and Holocene subtropical vegetation dynamics recorded in perched lake deposits on Fraser Island, Queensland, Australia. *Palaeogeography, Palaeoclimatology, Palaeoecology* **241**, 417–439.

Donders, T.H., Haberle, S.G., Hope, G., Wagner, F., Visscher, H., 2007. Pollen evidence for the transition of the Eastern Australian climate system from the post-glacial to the present-day ENSO mode. *Quaternary Science Reviews* **26**, 1621–1637.

Ellerton, D., Rittenour, T., Miot da Silva, G., Gontz, A., Shulmeister, J., Hesp, P., Santini, T., Welsh, K.J., 2018. Late-Holocene cliff-top blowout activation and evolution in the Cooloola Sand Mass, south-east Queensland, Australia. *The Holocene* **28**, 1697–1711.

Ellerton, D., Rittenour, T., Shulmeister, J., Gontz, A., Welsh, K.J., Patton N.R., 2020. An 800 kyr record of dune emplacement in relationship to high sea level forcing, Cooloola Sand Mass, Queensland, Australia. *Geomorphology* **354**, 106999.

Ellerton, D., Rittenour, T., Shulmeister, J., Roberts, A.P., Miot da Silva, G., Gontz, A., Hesp, P., et al., 2023. Fraser Island (K'gari) and initiation of the Great Barrier Reef linked by Middle Pleistocene sea-level change. *Nature Geoscience* **15**, 1017–1026.

Fensham, R.J., 1997. Aboriginal fire regimes in Queensland, Australia: analysis of the explorers' record. *Journal of Biogeography* **24**, 11–22.

Filion, L., 1984. A relationship between dunes, fire and climate recorded in the Holocene deposits of Quebec. *Nature* **309**, 543–546.

Filkov, A.I., Ngo, T., Matthews, S., Telfer, S., Penman, T.D., 2020. Impact of Australia's catastrophic 2019/20 bushfire season on communities and environment. Retrospective analysis and current trends. *Journal of Safety Science and Resilience* **1**, 44–56.

Fink, D., Hotchkis, M., Hua, Q., Jacobsen, G., Smith, A.M., Zoppi, U., Child, D., et al., 2004. The ANTARES AMS Facility at ANSTO. *Nuclear Instruments and Methods in Physics Research B* **223–224**, 109–115.

Fletcher, M.S., Hall, T., Alexandra, A.N., 2021. The loss of an Indigenous constructed landscape following British invasion of Australia: an insight into the deep human imprint on the Australian landscape. *Ambio* **50**, 138–149.

Gallagher, R.V., Allen, S., Mackenzie, B.D., Yates, C.J., Gosper, C.R., Keith, D.A., Merow, C., et al., 2021. High fire frequency and the impact of the 2019–2020 megafires on Australian plant diversity. *Diversity and Distributions* **27**, 1166–1179.

Gavin, D.G., Brubaker, L.B., Lertzman, K.P., 2003. An 1800-year record of the spatial and temporal distribution of fire from the west coast of Vancouver Island, Canada. *Canadian Journal of Forest Research* **33**, 573–586.

Gross, W., Morrill, C., Wahl, E., 2018. New advances at NOAA's World data service for paleoclimatology–Promoting the FAIR principles. *Past Global Changes Magazine* **26**(2), 58–58.

Hanson, J.M., VanderGragt, M.L., Welsh, K.J., Moss, P.T., 2022. Variations in wetland conditions within the Fitzroy Basin, north-eastern Australia: a palaeoecological approach. *Marine and Freshwater Research* **73**, 35–47.

Hanson, J.M., Welsh, K.J., Moss, P.T., Gadd, P., 2023. Implications of sea level variability on the formation and evolution of subtropical Rainbow Beach patterned fen complexes, Queensland, Australia. *The Holocene* **33**, 49–60.

Harrison, S.P., Villegas-Diaz, R., Cruz-Silva, E., Gallagher, D., Kesner, D., Lincoln, P., Shen, Y., et al., 2022. The Reading Palaeofire Database v1b: an expanded global resource to document changes in fire regimes from sedimentary charcoal records. *Earth System Science Data* **14**, 1109–1124.

Hawkins, P.J., 1975. Forest management of Cooloola State Forest. In: Kikkawa, J., Nix, H.A. (Eds), *Managing Terrestrial Ecosystems. Proceedings of the Ecological Society of Australia* **9**, 328–333.

Hawthorne, D., Mustaphi, C.J.C., Aleman, J.C., Blarquez, O., Colombaroli, D., Daniau, A.L., Marlon, J.R., et al., 2018. Global Modern Charcoal

Dataset (GMCD): a tool for exploring proxy-fire linkages and spatial patterns of biomass burning. *Quaternary International* **488**, 3–17.

Hennebelle, A., Aleman, J.C., Ali, A.A., Bergeron, Y., Carcaillet, C., Grondin, P., Landry, J., Blarquez, O., 2020. The reconstruction of burned area and fire severity using charcoal from boreal lake sediments. *The Holocene* **30**, 1400–1409.

Hennessy, K., Lucas, C., Nicholls, N., Bathols, J., Suppiah, R., Ricketts, J., 2005. *Climate Change Impacts on Fire-Weather in South-East Australia*. Climate Impacts Group, CSIRO Atmospheric Research and the Australian Government Bureau of Meteorology, Aspendale.

Hesse, P.P., 2016. How do longitudinal dunes respond to climate forcing? Insights from 25 years of luminescence dating of the Australian desert dunefields. *Quaternary International* **410**, 11–29.

Higuera, P.E., Sprugel, D.G., Brubaker, L.B., 2005. Reconstructing fire regimes with charcoal from small-hollow sediments: a calibration with tree-ring records of fire. *The Holocene* **15**, 238–251.

Higuera, P.E., Peters, M.E., Brubaker, L.B., Gavin, D.G., 2007. Understanding the origin and analysis of sediment-charcoal records with a simulation model. *Quaternary Science Reviews* **26**, 1790–1809.

Hogg, A.G., Heaton, T.J., Hua, Q., Palmer, J.G., Turney, C.S., Southon, J., Bayliss, A., et al., 2020. SHCal20 Southern Hemisphere calibration, 0–55,000 years cal. BP. *Radiocarbon* **62**, 759–778.

Houser, C., Wernette, P., Rentschlar, E., Jones, H., Hammond, B., Trimble, S., 2015. Post-storm beach and dune recovery: implications for barrier island resilience. *Geomorphology* **234**, 54–63.

Hua, Q., Jacobsen, G.E., Zoppi, U., Lawson, E.M., Williams, A.A., Smith, A.M., McGann, M.J., 2001. Progress in radiocarbon target preparation at the ANTARES AMS Centre. *Radiocarbon* **43**(2A) 275–282.

Hua, Q., Turnbull, J.C., Santos, G.M., Rakowski, A.Z., Ancapichún, S., De Pol-Holz, R., Hammer, S., et al., 2022. Atmospheric radiocarbon for the period 1950–2019. *Radiocarbon* **64**, 723–745.

Iglesias, V., Yospin, G.I., Whitlock, C., 2015. Reconstruction of fire regimes through integrated paleoecological proxy data and ecological modeling. *Frontiers in Plant Science* **5**, 785.

[IPCC] Intergovernmental Panel on Climate Change, 2021. *Climate Change 2021: The Physical Science Basis*. Contribution of Working Group I to the Sixth Assessment Report of the Intergovernmental Panel on Climate Change. Cambridge University Press, Cambridge.

Itter, M.S., Finley, A.O., Hooten, M.B., Higuera, P.E., Marlon, J.R., Kelly, R., McLachlan, J.S., 2017. A model-based approach to wildland fire reconstruction using sediment charcoal records. *Environmetrics* **28**, e2450.

Käyhkö, J.A., Worsley, P., Pye, K., Clarke, M.L., 1999. A revised chronology for aeolian activity in subarctic Fennoscandia during the Holocene. *The Holocene* **9**, 195–205.

Keeley, J.E., 1995. Seed-germination patterns in fire-prone Mediterranean-climate regions. In: Arroyo, M.T.K., Zedler, P.H., Fox, M.D. (Eds.), *Ecology and Biogeography of Mediterranean Ecosystems in Chile, California, and Australia*. Springer, New York, pp. 239–273.

Keith, D., 2004. *Ocean Shores to Desert Dunes: The Native Vegetation of New South Wales and the ACT*. Department of Environment and Conservation, Hurstville, NSW, Australia.

Kemp, C., Tibby, J., Barr, C., Arnold, L., 2021. Climate, fire and vegetation history from subtropical North Stradbroke Island (Minjerribah), eastern Australia, during the last three interglacials. *Journal of Quaternary Science* **36**, 1201–1213.

Kershaw, A.P., 1986. Climatic change and Aboriginal burning in north-east Australia during the last two glacial/interglacial cycles. *Nature* **322**, 47–49.

Kershaw, A.P., Clark, J.S., Gill, A.M., D'Costa, D.M., 2002. A history of fire in Australia. In: Bradstock, R.A., Williams, J.E., Gill, A.M. (Eds.), *Flammable Australia: The Fire Regimes and Biodiversity of a Continent*. Cambridge University Press, Cambridge, pp. 3–25.

Köhler, M., Shulmeister, J., Patton, N.R., Rittenour, T.M., McSweeney, S., Ellerton, D.T., Hüneke, H., 2021. Holocene evolution of a barrier-spit complex and the interaction of tidal and wave processes, Inskip Peninsula, SE Queensland, Australia. *The Holocene* **31**, 1476–1488.

Krishnan, V., Robinson, N., Firn, J., Applegate, G., Herbohn, J., Schmidt, S., 2018. Without management interventions, endemic wet-sclerophyll

forest is transitioning to rainforest in World Heritage listed K'gari (Fraser Island), Australia. *Ecology and Evolution* **9**, 1378–1393.

Lancaster, N., Wolfe, S., Thomas, D., Bristow, C., Bubenzer, O., Burrough, S., Duller, G., et al., 2016. The INQUA Dunes Atlas chronologic database. *Quaternary International* **410**, 3–10.

Lees, B., 2006. Timing and formation of coastal dunes in northern and eastern Australia. *Journal of Coastal Research* **22**, 78–89.

Levin, N., 2011. Climate-driven changes in tropical cyclone intensity shape dune activity on Earth's largest sand island. *Geomorphology* **125**, 239–252.

Levin, N., Levental, S., Morag, H., 2012. The effect of wildfires on vegetation cover and dune activity in Australia's desert dunes: a multisensor analysis. *International Journal of Wildland Fire* **21**, 459–475.

Levin, N., Jablon, P.E., Phinn, S., Collins, K., 2017. Coastal dune activity and foredune formation on Moreton Island, Australia, 1944–2015. *Aeolian Research* **25**, 107–121.

Lewis, S.E., Wüst, R.A., Webster, J.M., Shields, G.A., 2008. Mid-late Holocene sea-level variability in eastern Australia. *Terra Nova* **20**, 74–81.

Leys, B.A., Commerford, J.L., McLauchlan, K.K., 2017. Reconstructing grassland fire history using sedimentary charcoal: considering count, size and shape. *PLoS ONE* **12**, e0176445.

Leys, B.A., Marlon, J.R., Umbanhowar, C., Vannière, B., 2018. Global fire history of grassland biomes. *Ecology and Evolution* **8**, 8831–8852.

Long, C.J., Whitlock, C., Bartlein, P.J., Millspaugh, S.H., 1998. A 9000-year fire history from the Oregon Coast Range, based on a high-resolution charcoal study. *Canadian Journal of Forest Research* **28**, 774–787.

Mann, D.H., Heiser, P.A., Finney, B.P., 2002. Holocene history of the Great Kobuk sand dunes, northwestern Alaska. *Quaternary Science Reviews* **21**, 709–731.

Mariani, M., Tibby, J., Barr, C., Moss, P., Marshall, J.C., McGregor, G.B., 2019. Reduced rainfall drives biomass limitation of long-term fire activity in Australia's subtropical sclerophyll forests. *Journal of Biogeography*, **46**, 1974–1987.

Mariani, M., Connor, S.E., Theuerkauf, M., Herbert, A., Kuneš, P., Bowman, D., Fletcher, M.S., et al., 2022. Disruption of cultural burning promotes shrub encroachment and unprecedented wildfires. *Frontiers in Ecology and the Environment* **20**, 292–300.

Marlon, J., Bartlein, P.J., Whitlock, C., 2006. Fire-fuel-climate linkages in the northwestern USA during the Holocene. *The Holocene* **16**, 1059–1071.

Marlon, J.R., Kelly, R., Daniau, A.L., Vannière, B., Power, M.J., Bartlein, P., Higuera, P., et al., 2015. Reconstructions of biomass burning from sediment-charcoal records to improve data–model comparisons. *Biogeosciences* **13**, 3225–3244.

Matthews, J.A., Seppälä, M., 2014. Holocene environmental change in subarctic aeolian dune fields: the chronology of sand dune re-activation events in relation to forest fires, palaeosol development and climatic variations in Finnish Lapland. *The Holocene* **24**, 149–164.

Maxson, C., Tibby, J., Marshall, J., Kent, M., Tyler, J., Barr, C., McGregor, G., Cadd, H., Schulz, C. Lomax, B.H., 2021. Fourier transform infrared spectroscopy as a tracer of organic matter sources in lake sediments. *Palaeogeography, Palaeoclimatology, Palaeoecology* **581**, 110622.

McKenzie, D., Gedalof, Z., Peterson, D., Mote, P., 2004. Climatic change, wildfire and conservation. *Conservation Biology* **18**, 890–902.

McLauchlan, K.K., Higuera, P.E., Miesel, J., Rogers, B.M., Schweitzer, J., Shuman, J.K., Tepley, A.J., et al., 2020. Fire as a fundamental ecological process: research advances and frontiers. *Journal of Ecology* **108**, 2047–2069.

McNiven, I.J., 1991. Teewah Beach: new evidence for Holocene coastal occupation in southeast Queensland. *Australian Archaeology* **33**, 14–27.

Mooney, S.D., Harrison, S.P., Bartlein, P.J., Daniau, A.-L., Stevenson, J., Brownlie, K.C., Buckman, S., et al., 2011. Late Quaternary fire regimes of Australasia. *Quaternary Science Reviews* **30**, 28–46.

Morris, J.L., Higuera, P.E., Haberle, S., Whitlock, C., 2017. Modern pollen from small hollows reflects *Athrotaxis cupressoides* density across a wildfire gradient in subalpine forests of the Central Plateau, Tasmania, Australia. *The Holocene* **27**, 1781–1788.

Moss, P., Mackenzie, L., Ulm, S., Sloss, C., Rosendahl, D., Petherick, L., Steinberger, L., Wallis, L., Heijnis, H., Petchey, F., Jacobsen, G., 2015. Environmental context for late Holocene human occupation of the South

Wellesley Archipelago, Gulf of Carpentaria, northern Australia. *Quaternary International* **385**, 136–144.

Moss, P.T., 2014. *Investigation of the Vegetation and Fire History of the EPBC, RAMSAR and WHA Wetlands of the Great Sandy Strait* (Unpublished report). University of Queensland, Brisbane, Australia.

Moss, P.T., Kershaw, P.A., 2000. The last glacial cycle from the humid tropics of northeastern Australia: comparison of a terrestrial and a marine record. *Palaeogeography, Palaeoclimatology, Palaeoecology* **155**, 155–176, 162–176.

Moss, P.T., Petherick, L., Neil, D., 2011. Environmental change at Myora Springs, North Stradbroke Island over the last millennium. *Proceedings of the Royal Society of Queensland* **117**, 133–140.

Moss, P.T., Tibby, J., Petherick, L., McGowan, H., Barr, C., 2013. Late Quaternary vegetation history of North Stradbroke Island, Queensland, eastern Australia. *Quaternary Science Reviews* **74**, 257–272.

Moy, C.M., Seltzer, G.O., Rodbell, D.T., Anderson, D. M., 2002. Variability of El Niño/Southern Oscillation activity at millennial timescales during the Holocene epoch. *Nature* **420**, 162–165.

Mulholland, C., 2021. Fighting to save an international icon—K'gari (Fraser Island). *Australian Journal of Emergency Management* **36**, 40–43.

Neal, R., Stock, E., 1986. Pleistocene occupation in the south-east Queensland coastal region. *Nature* **323**, 618–621.

Ngugi, M.R., Knight, J., Hua, Q., Dowling, R., Kington, D., Burns, D., 2020. Ageing culturally significant relic trees in southeast Queensland to support bushfire management strategies. *Ecological Management Restoration* **21**, 147–150.

Patton, N.R., Ellerton, D., Shulmeister, J., 2019. High-resolution remapping of the coastal dune fields of south east Queensland, Australia: a morphometric approach. *Journal of Maps* **15**, 578–589.

Patton, N.R., Shulmeister, J., Ellerton, D., Seropian, G., 2022a. Measuring landscape evolution from inception to maturity: insights from a coastal dune system. *Earth and Planetary Science Letters* **584**, 117448.

Patton, N.R., Shulmeister, J., Rittenour, M.T., Almond, P., Ellerton, D.T., Santini T., 2022b. Using calibrated surface roughness dating to estimate coastal dune ages at K'gari (Fraser Island) and the Cooloola Sand Mass, Australia. *Earth Surface Processes and Landforms* **47**, 2455–2470.

Peel, M.C., Finlayson, B.L., McMahon, T.A., 2007. Updated world map of the Köppen-Geiger climate classification. *Hydrology and Earth System Sciences* **11**, 1633–1644.

Power, M.J., Marlon, J., Ortiz, N., Bartlein, P.J., Harrison, S.P., Mayle, F.E., Ballouche, A., *et al.*, 2008. Changes in fire regimes since the Last Glacial Maximum: an assessment based on a global synthesis and analysis of charcoal data. *Climate Dynamics* **30**, 887–907.

Pyne S.J., 1998. *Burning Bush: A Fire History of Australia*. Henry Holt, New York.

Queensland Herbarium, 2021. Regional Ecosystem Description Database (REDD). Version 12.1. Queensland Department of Environment and Science, Brisbane (accessed April 1, 2022). www.qld.gov.au/environment/plants-animals/plants/ecosystems.

R Core Team, 2020. *R: A Language and Environment for Statistical Computing*. R Foundation for Statistical Computing, Vienna, Austria. www.R-project.org.

Reeve, R., Fergus, I.F., Thompson, C.H., 1985. Studies in landscape dynamics in the Cooloola-Noosa River area, Queensland. 4. Hydrology and water chemistry. In: *CSIRO Australia, Division of Soils Divisional Report No. 77*. CSIRO, St. Lucia, QLD, pp. 1–42. https://doi.org/10.25919/5c8fdcd51bd55.

Reid, L.M., Dunne, T., 1996. *Rapid Evaluation of Sediment Budgets*. Vol. 29. Catena, Reiskirchen, Germany.

Remy, C.C., Fouquemberg, C., Asselin, H., Andrieux, B., Magnan, G., Brossier, B., Grondin, P., *et al.*, 2018. Guidelines for the use and interpretation of palaeofire reconstructions based on various archives and proxies. *Quaternary Science Reviews* **193**, 312–322.

Richards, L., Brew, N., Smith, L., 2020. *2019–2020 Australian Bushfires—Frequently Asked Questions: A Quick Guide*. Parliament of Australia, Research Paper Series 2019–2020 (accessed June 2, 2020). www.aph.gov.au/About_Parliament/Parliamentary_Departments/Parliamentary_Library/pubs/rp/rp1920/Quick_Guides/AustralianBushfires.

Roering, J.J., Gerber, M., 2005. Fire and the evolution of steep, soil-mantled landscapes. *Geology* **33**, 349–352.

Roering, J.J., Kirchner, J.W., Dietrich, W.E., 1999. Evidence for nonlinear, diffusive sediment transport on hillslopes and implications for landscape morphology. *Water Resources Research* **35**, 853–870.

Russell-Smith, J., Lucas, D., Gapindi, M., Gunbunuka, B., Kapirigi, N., Namingum, G., Lucas, K., Giuliani, P., Chaloupka, G., 1997. Aboriginal resource utilization and fire management practice in western Arnhem Land, monsoonal northern Australia: notes for prehistory, lessons for the future. *Human Ecology* **25**, 159–195.

Russell-Smith, J., Yates, C.P., Whitehead, P.J., Smith, R., Craig, R., Allan, G.E., Thackway, R., *et al.*, 2007. Bushfires "down under": patterns and implications of contemporary Australian landscape burning. *International Journal of Wildland Fire* **16**, 361–377.

Sadler, P.M., 1981. Sediment accumulation rates and the completeness of stratigraphic sections. *Journal of Geology* **89**, 569–584.

Sanborn, P., Geertsema, M., Jull, A.J.T., Hawkes, B., 2006. Soil and sedimentary charcoal evidence for Holocene forest fires in an inland temperate rainforest, east-central British Columbia, Canada. *The Holocene* **16**, 415–427.

Schmieder, J., Fritz, S.C., Grimm, E.C., Jacobs, K.C., Brown, K.J., Swinehart, J.B., Porter, S.C., 2013. Holocene variability in hydrology, vegetation, fire, and eolian activity in the Nebraska Sand Hills, USA. *The Holocene* **23**, 515–527.

Schoenberger, P.J., Wysocki, D.A., Benham, E.C., Broderson, W.D., 2002. *Field Book for Describing and Sampling Soils*. Version 2.0. Natural Resources Conservation Service, National Soil Survey Center, Lincoln, NE.

Schreuder, L.T., Donders, T.H., Mets, A., Hopmans, E.C., Damsté, J.S.S., Schouten, S., 2019. Comparison of organic and palynological proxies for biomass burning and vegetation in a lacustrine sediment record (Lake Allom, Fraser Island, Australia. *Organic Geochemistry* **133**, 10–19.

Seppälä, M., 1995. Deflation and redeposition of sand dunes in Finnish Lapland. *Quaternary Science Reviews* **14**, 799–809.

Shakesby, R.A., Doerr, S.H., 2006. Wildfire as a hydrological and geomorphological agent. *Earth-Science Reviews* **74**, 269–307.

Shulmeister, J., Lees, B.G., 1995. Pollen evidence from tropical Australia for the onset of an ENSO-dominated climate at c. 4000 BP. *The Holocene* **5**, 10–18.

Shumack, S., Hesse, P., 2018. Assessing the geomorphic disturbance from fires on coastal dunes near Esperance, Western Australia: implications for dune de-stabilisation. *Aeolian Research* **31**, 29–49.

Shumack, S., Hesse, P., Turner, L., 2017. The impact of fire on sand dune stability: surface coverage and biomass recovery after fires on Western Australian coastal dune systems from 1988 to 2016. *Geomorphology* **299**, 39–53.

Singh, G., Kershaw, A.P., Clark, R., 1981. Quaternary vegetation and fire history in Australia. In: Gill, A.M., Groves, R.H., Noble, I.R. (Eds.), *Fire and the Australian Biota*. Australian Academy of Science, Canberra, pp. 23–54.

Sorensen, L., 2007. A Spatial Analysis Approach to Global Delineation of Dryland Area of Relevance to CBD Programme of Work on Dry and Subhumid Lands. UNEP-WCMC, Cambridge, UK (accessed May 22, 2022). http://datadownload.unep-wcmc.org/datasets.

Spencer, R.J., Baxter, G.S., 2006. Effects of fire on the structure and composition of open eucalypt forests. *Austral Ecology* **31**, 638–646.

Srivastava, S.K., King, L., Mitchell, C., Wiegand, A., Carter, R.W., Shapcott, A., Russell-Smith, J., 2012. Ecological implications of standard fire-mapping approaches for fire management of the World Heritage Area, Fraser Island, Australia. *International Journal of Wildland Fire* **22**, 381–393.

Stone, Z.L., Maron, M., Tasker, E., 2022. Reduced fire frequency over three decades hastens loss of the grassy forest habitat of an endangered songbird. *Biological Conservation* **270**, 109570.

Tejan-Kella, M.S., Chittleborough, D.J., Fitzpatrick, R.W., Thompson, C.H., Prescott, J.R., Hutton, J.T., 1990. Thermoluminescence dating of coastal sand dunes at Cooloola and North Stradbroke Island, Australia. *Soil Research* **28**, 465–481.

Thomas, A., 2003. *Fraser Island World Heritage Area Fire Management Systems: Fire Strategy*. Queensland Government, Queensland Parks and Wildlife Service, Brisbane.

Thomas, D.S., Wiggs, G.F., 2008. Aeolian system responses to global change: challenges of scale, process and temporal integration. *Earth Surface Processes and Landforms* **33**, 1396–1418.

Thompson, C.H., 1981. Podzol chronosequences on coastal dunes of eastern Australia. *Nature* **291**, 59–61.

Thompson, C.H., 1983. Development and weathering of large parabolic dune systems along the subtropical coast of Eastern Australia. *Zeitschrift fuer Geomophologie*, Suppl. 45, 205–225.

Thompson, C.H., 1992. Genesis of podzols on coastal dunes in southern Queensland. Field relationships and profile morphology. *Soil Research* **30**, 593–613.

Thompson, C.H., Moore, A.W., 1984. Studies in landscape dynamics in the Cooloola-Noosa River area, Queensland. 1. Introduction, general description and research approach. *CSIRO Australia, Division of Soils Divisional Report No. 73*. CSIRO, St. Lucia, QLD, pp. 1–93. https://doi.org/10.25919/5c8fdcef11537.

Turney, C.S., Kershaw, A.P., Moss, P., Bird, M.I., Fifield, L.K., Cresswell, R.G., *et al.*, 2001. Redating the onset of burning at Lynch's Crater (North Queensland): implications for human settlement in Australia. *Journal of Quaternary Science* **16**, 767–771.

[UNESCO] United Nations Educational, Scientific and Cultural Organization World Heritage Convention, 2021. K'gari (Fraser Island) listing (accessed January 1, 2022). https://whc.unesco.org/en/list/630/

Vachula, R.S., Russell, J.M., Huang, Y., Richter, N., 2018. Assessing the spatial fidelity of sedimentary charcoal size fractions as fire history proxies with a high-resolution sediment record and historical data. *Palaeogeography, Palaeoclimatology, Palaeoecology* **508**, 166–175.

Vachula, R.S., Sheppard, R.Y., Cheung, A.H., 2022. Preservation biases are pervasive in Holocene paleofire records. *Palaeogeography, Palaeoclimatology, Palaeoecology* **602**, 111165.

van der Werf, G.R., Randerson, J.T., Giglio, L., van Leeuwen, T.T., Chen, Y., Rogers, B.M., Mu, M., *et al.*, 2017. Global fire emissions estimates during 1997–2016. *Earth System Science Data* **9**, 697–720.

Walker, J., Thompson, C.H., Fergus, I.F., Tunstall, B.R., 1981. Plant succession and soil development in coastal sand dunes of subtropical eastern Australia. In: West, D.C., Shugart, H.H., Botkin, D.B. (Eds.), *Forest Succession*. Springer, New York, pp. 107–131.

Walker, J., Thompson, C.H., Lacey, C.J., 1987. Morphological differences in lignotubers of *Eucalyptus intermedia* RT Bak. and *E. signata* F. Muell. associated with different stages of podzol development on coastal dunes, Cooloola, Queensland. *Australian Journal of Botany* **35**, 301–311.

Walker, J., Lees, B., Olley, J., Thompson, C., 2018. Dating the Cooloola coastal dunes of south-eastern Queensland, Australia. *Marine Geology* **398**, 73–85.

Walker, L.R., Wardle, D.A., Bardgett, R.D., Clarkson, B.D., 2010. The use of chronosequences in studies of ecological succession and soil development. *Journal of Ecology* **98**, 725–736.

Ward, W.T., 2006. Coastal dunes and strandplains in southeast Queensland: sequence and chronology. *Australian Journal of Earth Sciences* **53**, 363–373.

Whitlock, C., Millspaugh, S.H., 1996. Testing assumptions of fire history studies: an examination of modern charcoal accumulation in Yellowstone National Park. *The Holocene* **6**, 7–15.

Whitlock, C., Larsen, C., 2001. Charcoal as a fire proxy. In: Smol, J.P., Birks, H.J.B., Last, W.M., Bradley, R.S., Alverson, K. (Eds.), *Tracking Environmental Change Using Lake Sediments*. Developments in Paleoenvironmental Research 3. Springer, Dordrecht, Netherlands, pp. 75–97.

Williams, A.N., Mooney, S.D., Sisson, S.A., Marlon, J., 2015. Exploring the relationship between Aboriginal population indices and fire in Australia over the last 20,000 years. *Palaeogeography, Palaeoclimatology, Palaeoecology* **432**, 49–57.